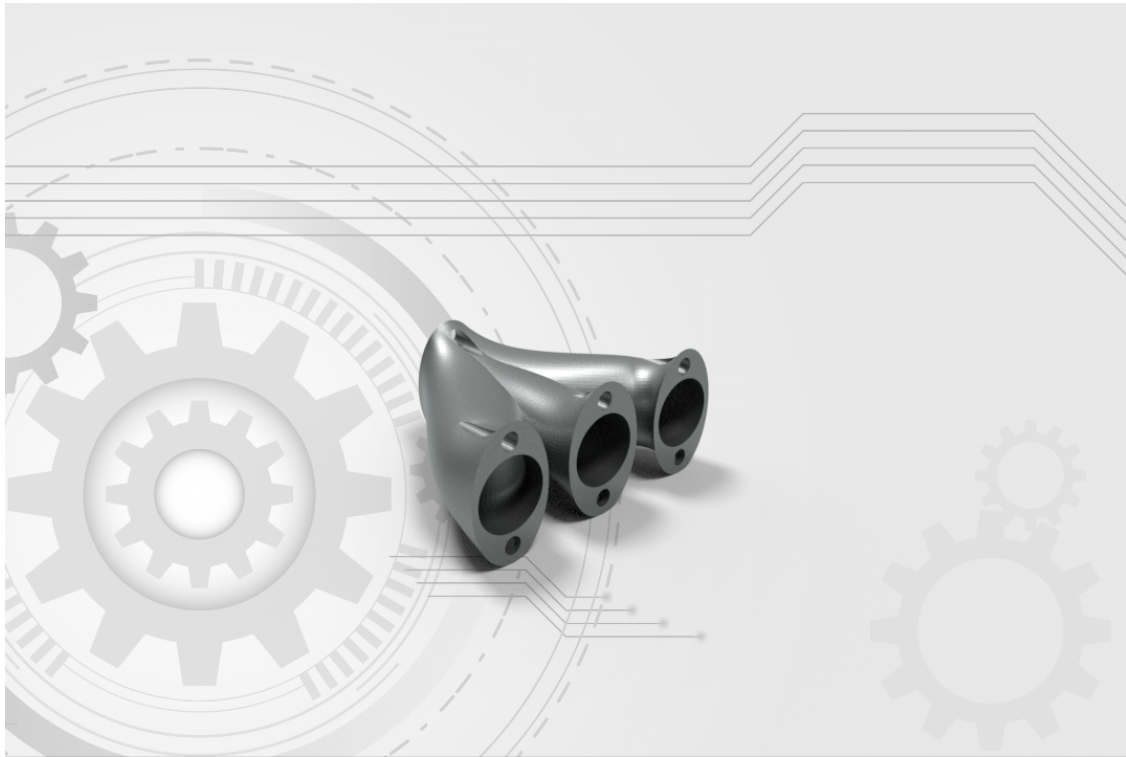




**CHALMERS**  
UNIVERSITY OF TECHNOLOGY



# **Design of a gas manifold for high pressure applications by Powder Bed Fusion – Laser Beam**

Master's thesis in Product Development

CHRISTOS LIATIS

SRI SAI SUMANTH PENDYALA

**DEPARTMENT OF INDUSTRIAL AND MATERIALS SCIENCE**

CHALMERS UNIVERSITY OF TECHNOLOGY

Gothenburg, Sweden 2023

[www.chalmers.se](http://www.chalmers.se)



MASTER'S THESIS 2023

**Design of a gas manifold for high pressure  
applications by Powder Bed Fusion – Laser Beam**

Christos Liatis

Sri Sai Sumanth Pendyala



**CHALMERS**  
UNIVERSITY OF TECHNOLOGY

Department of Industrial and Materials Science  
CHALMERS UNIVERSITY OF TECHNOLOGY  
Gothenburg, Sweden 2023

Design of a gas manifold for high pressure applications by Powder Bed Fusion –  
Laser Beam

Christos Liatis

Sri Sai Sumanth Pendyala

© Christos Liatis, 2023.

© Sri Sai Sumanth Pendyala, 2023.

Supervisor A: James Shipley, Quintus Technologies

Supervisor B: Rasmus Gunnerek, Materials and manufacturing

Examiner: Eduard Hryha, Materials and manufacturing

Master's Thesis 2023

Department of Industrial and Materials Science

Chalmers University of Technology

SE-412 96 Gothenburg

Telephone +46 31 772 1000

Cover: Gas Manifold designed for AM.

Cover background image taken from [www.freepic.com](http://www.freepic.com)

Typeset in L<sup>A</sup>T<sub>E</sub>X

Printed by Chalmers Reproservice

Gothenburg, Sweden 2023

# Abstract

This thesis report was conducted in the Product Development Master's Program at Chalmers University of Technology. The project is related to Powder Bed Fusion - Laser Beam, an Additive Manufacturing technology and how its productivity can increase. The report intends to present which printing parameters one can take advantage of, to enable high build rates using the specific technology. The perspective of high productivity was one of the main factors that affected the result of the project since it plays a vital role in modern industry and how attractive AM can be. The whole research was in collaboration with Quintus Technologies, a firm located in Västerås that focuses on Hot Isostatic Pressing equipment design and manufacture.

The component that the project was concentrated on was a gas manifold, as an idea for practical usage in Quintus Technologies. The research was initiated by conducting a Generative Flow Analysis aiming to optimize the flow of the manifold and followed by 3D-Modelling. The manifold was designed for AM to account for satisfactory buildability and following post-AM process, HIP. In other words, design iterations needed to be executed since the printing process should be with minimal support structures, aiming in decreasing lead time through reduction in post-processing. Materialise Magics software was used to examine what kind of support structures are necessary and in which spots they are needed. To accomplish this, each design was placed in different orientations and found out the best orientation possible for printing this manifold.

Additionally, the trade-off between printing time and density is discussed since controlling porosity levels can contribute to increasing productivity. An attempt of predicting the densification levels in the manifold but also in simpler geometries after HIP was conducted using Simufact Additive software. Occurred errors during the calculations are discussed further in the respective sections.

Every difficulty that occurred during the process of the project is described in detail. This work aims to be a steppingstone towards AM industrialization and enable mass production.

**Keywords:** Powder Based Fusion - Laser Beam, Gas Manifold, Design for Additive Manufacturing, High Productivity, Hot Isostatic Pressing.



# Acknowledgements

To begin with, we are grateful for the help offered by our supervisor James Shipley, the Manager for Global Business Development for Advanced Material Densification at Quintus Technologies. He assisted us with his ideas and suggestions throughout the research and he provided us with advice and connections in order to enrich our knowledge database. Although he was travelling a lot, he was always trying to find some time for us and contribute to our project.

We would like to thank Anders Magnusson, the Business Development Manager of Quintus. Anders facilitated us by enriching our knowledge regarding HIP and contributed a lot to this research giving us specific data about Quintus equipment. We appreciate James and Anders for showing us the company facilities, when we visited the company headquarters in Västerås. Also, we appreciate the way they treated us, making us feel that we belong to Quintus Family even if we worked remotely.

Additionally, we want to thank our supervisor Rasmus Gunnerek and our examiner Eduard Hryha. Rasmus played a significant role during the project since he was always present and he helped us in every step of our thesis. We are grateful for his advice, comments, and guidance during this research. As for Eduard, nothing would have happened without him since he connected us with Quintus Technologies. We thank him for his willingness to help whenever we needed it and for his warm welcome in the Centre of Additive Manufacture - Metals.

Finally, it is important for us to thank our friends, partners, and families for their immeasurable support and patience during this master thesis project.

**Christos Liatis, Sri Sai Sumanth Pendyala**  
Gothenburg, June 2023



# List of Acronyms

The list of acronyms used throughout this thesis are presented in the alphabetical order:

AM	Additive Manufacturing
CAD	Computer Aided-Design
GFA	Generative Flow Analysis
HIP	Hot Isostatic Pressing
LoF	Lack of Fusion
PBF-LB	Powder Based Fusion-Laser Beam
SS	Stainless Steel



# Contents

<b>List of Acronyms</b>	<b>ix</b>
<b>List of Figures</b>	<b>xiii</b>
<b>List of Tables</b>	<b>xv</b>
<b>1 Introduction</b>	<b>1</b>
1.1 Background . . . . .	1
1.2 Problem Statement . . . . .	2
1.3 Purpose . . . . .	3
1.4 Aim . . . . .	3
1.5 Scope of the thesis . . . . .	3
1.6 Research questions . . . . .	3
1.7 Report outline . . . . .	4
<b>2 Theory and Literature Review</b>	<b>5</b>
2.1 Additive manufacturing . . . . .	5
2.1.1 Powder Bed Fusion – Laser Beam . . . . .	5
2.1.2 Design Process for AM . . . . .	7
2.1.3 Materials in PBF-LB and 316L Stainless Steel . . . . .	8
2.1.4 Advantages and Limitations . . . . .	9
2.1.5 Porosity effects on AM component . . . . .	10
2.1.6 Recoating time . . . . .	10
2.2 Hot Isostatic Pressing . . . . .	10
2.2.1 Simulation of Hot Isostatic Pressing . . . . .	13
<b>3 Methodology</b>	<b>15</b>
3.1 Research Design . . . . .	15
3.2 Generative Flow Analysis . . . . .	16
3.3 Design for AM . . . . .	18
3.4 Simulations . . . . .	18
3.4.1 Challenges during simulations . . . . .	20
3.5 Different Porosity Levels . . . . .	20
<b>4 Results and Discussion</b>	<b>23</b>
4.1 Preliminary Design . . . . .	23
4.1.1 Manifold Design - Generative Flow Analysis 1 . . . . .	23

4.1.2	CAD design . . . . .	24
4.2	Iterations . . . . .	25
4.2.1	Manifold Design - Generative Flow Analysis 2 . . . . .	25
4.2.2	Comparison for GFA 1 and GFA 2 . . . . .	26
4.2.3	CAD design . . . . .	27
4.2.4	Design 3 . . . . .	28
4.3	Final Design - Analysis . . . . .	29
4.4	Simulations . . . . .	30
4.4.1	Simulations of HIP on gas manifold . . . . .	30
4.4.2	Cylinder simulations . . . . .	31
<b>5</b>	<b>Conclusion and Future Work</b>	<b>35</b>
5.1	Contributions of the Study . . . . .	35
5.2	Summary of Key Findings . . . . .	35
5.3	Future Work . . . . .	36
	<b>Bibliography</b>	<b>39</b>
<b>A</b>	<b>Appendix - Design characteristics</b>	<b>I</b>
<b>B</b>	<b>Appendix - Build Orientations</b>	<b>III</b>
<b>C</b>	<b>Appendix - GFA - 2</b>	<b>V</b>
<b>D</b>	<b>Appendix - Build Orientations</b>	<b>VII</b>

# List of Figures

1	Schematic representation of the PBF-LB Process inspired by [19] . . .	6
2	Maximum service temperature vs Young’s modulus graph . . . . .	8
3	HIP Cycle Graph . . . . .	11
4	Schematic figure of the Hot Isostatic Pressing process . . . . .	12
5	Process Framework . . . . .	15
6	Generative Flow Analysis (a) Block model Version 1 isometric view (b) Block model Version 2 isometric view . . . . .	16
7	Thermal Properties for SS 316L (a) Thermal Conductivity/Temper- ature (b) Specific heat capacity/Temperature . . . . .	19
8	(a) Temperature Time Graph (b) Pressure Time Graph . . . . .	20
9	GFA-1 Models (a) Model 1 (b) Model 2 . . . . .	23
10	(a) Velocity Magnitude (b) Pressure Reference . . . . .	24
11	Manifold Design 1 (a) Rear view (b) Front view . . . . .	24
12	Final model of fluid flow . . . . .	25
13	Final model flow analysis (a) Pressure reference (b) velocity magnitude	26
14	Specification comparison of GFA-1 and GFA-2 . . . . .	26
15	Manifold Design 2 (a) Rear View (b) Front View . . . . .	27
16	Manifold Design 3 (a) Rear View (b) Front view . . . . .	28
17	Manifold Design 3 (a) Outer Supports (b) Inner Supports . . . . .	28
18	Manifold Design 4 (a) Rear View (b) Front view . . . . .	29
19	Manifold Design 4 (a) Solid view (b) Transparent view . . . . .	29
20	Design for AM Progress . . . . .	30
21	Manifold Simulations (a) 99% initial density, front view (b) 99% ini- tial density, rear view (c) 67.5% initial density, front view (d) 67.5% initial density, rear view . . . . .	31
22	Relative density Results (a) First cylinder (b) Second cylinder printed vertically (c) Second cylinder printed horizontally . . . . .	32
23	Design Iterations-Dimensions . . . . .	I
24	(a) 1st orientation, Outer supports (b) 1st orientation, Inner supports (c) 2nd orientation, Outer supports (d) 2nd orientation, Inner sup- ports (e) 3rd orientation, Outer supports (f) 3rd orientation, Inner supports . . . . .	III

25	(g) 4th orientation, Outer supports (h) 4th orientation, Inner supports (i) 5th orientation, Outer supports (j) 5th orientation, Inner supports . . . . .	IV
26	Manifold GFA-2 Multiple Angles (a) 1st angle (b) 2nd angle (c) 3rd angle . . . . .	V
27	(a) 1st orientation, Outer supports (b) 1st orientation, Inner supports (c) 2nd orientation, Outer supports (d) 2nd orientation, Inner supports (e) 3rd orientation, Outer supports (f) 3rd orientation, Inner supports . . . . .	VII
28	(a) 1st orientation, Outer supports (b) 1st orientation, Inner supports (c) 2nd orientation, Outer supports (d) 2nd orientation, Inner supports (e) 3rd orientation, Outer supports (f) 3rd orientation, Inner supports . . . . .	VIII

# List of Tables

1	Requirement list for manifold . . . . .	16
2	Constraint codes for colors . . . . .	17
3	Composition of SS 316L . . . . .	19
5	Densification Calculation Parameters . . . . .	19
4	HIP Parameters . . . . .	20



# 1

## Introduction

*This chapter presents the context and objectives of the master thesis that are introduced, alongside its scope and constraints. The research topic is contextualized within the industry, highlighting its importance and the difficulties it aims to tackle. This master's thesis is a collaborative effort with Quintus Technologies, a Kobelco Group company, based in Västerås, Sweden, and in the frame of Centre of Additive Manufacturing - Metal CAM<sup>2</sup>, hosted by Chalmers University.*

### 1.1 Background

There is a growing demand for Additive Manufacturing (AM) in various industries due to its potential to manufacture complex geometries, cut lead times, and optimize material utilization which is costly or not possible by conventional manufacturing processes such as drilling, milling, and CNC machining. In addition to this, AM enables industries to produce tailor-made spare parts, a fact that can lead to inventory reduction [1]. In other words, logistics issue decreases while the industry's capital is being used more effectively. Numerous developments over the years, such as improved quality or decreased production lead times, have helped AM develop and become more competitive compared with traditional manufacturing routes.

Though it has many advantages, AM faces a significant challenge in its widespread adoption due to the relatively high costs compared to traditional manufacturing [2]. The expenses arise from various factors, starting with the specialized equipment required, such as 3D printers which are complex machines. These machines often incorporate advanced technologies and precision components, leading to substantial price tags [3]. Not only printers but also printable material can be costly [4]. The materials used in AM, including metal powders or high-performance polymers, tend to be more expensive compared to traditional manufacturing materials per kilo, however, less material is most often used.

Furthermore, AM technologies can offer products of complex geometry or the option for higher productivity, but the trade-off is the loss of quality in the part [5]. Thus, post-processing steps often prove essential, with printed parts requiring treatments such as polishing, heat treatment, or surface finishing, all of which delay the product development and manufacturing lead time, leading in turn to increasing overall expenses. Another disadvantage of these technologies is that support structures are

often needed. On the one hand, they are necessary for supporting overhung sections, distributing heat, or decreasing residual stresses [6]. However, they constitute one of the main reasons for decreasing productivity of AM overall [7]. Low productivity is a serious disadvantage that contributes to AM's high expenses. At the time of this research, AM is significantly less productive than conventional methods when the build rate and the overall processing of components are considered [8]. Moreover, the complex nature of AM processes demands skilled expertise, technical knowledge, and educational programs [9]. These aspects result in overall higher manufacturing costs.

The combined impact of these cost factors presents a challenge for businesses, particularly those with limited budgets or high-volume production requirements. The perceived high costs of AM may deter companies from fully embracing the technology and realizing its vast potential [10]. However, ongoing advancements in the field are aimed at mass production and reducing costs by optimizing processes, improving material efficiency, and exploring alternative materials. As these efforts continue, it is expected that AM will become more economically feasible, enabling wider adoption across industries.

Powder Bed Fusion - Laser Beam (PBF-LB) is considered to be one of the few AM technologies to support higher build rates (refer Subsection 2.1.1). To maintain acceptable quality and mechanical properties of PBF-LB manufactured components, the build speed is kept low which makes it more expensive than conventional manufacturing methods. To increase the build speed and hence productivity, there are some parameters that can be adjusted accordingly such as the laser power, scan speed, hatch distance, and layer thickness [11]. However, there are many other parameters that can affect the process. Post-processing techniques like Hot Isostatic Pressing (HIP) can complement well with PBF-LB for better efficiency to counteract those defects in the components ensuring full density and better mechanical properties.

## 1.2 Problem Statement

Researchers have explored different approaches [12][7] to counteract the expensive resource aspect of PBF-LB. One of those is to increase productivity and handle printing parameters in a way, so that time and materials are saved reducing the process cost consequentially. Identifying the important factors that play a vital role in printing time and build rates is a task to be performed. Therefore, this research is crucial for the evolution of additive manufacturing and its attractiveness to investors in the future.

Considering the equipment of Quintus facilities, it consists of some components that need optimization in terms of material usage and functionality. At present, the component that is considered is a gas manifold that is manufactured using conventional methods like drilling and machining. The problem statement is how can the design

for AM used to create and print this manifold in order to be used in their equipment for efficient usage of the resources.

### **1.3 Purpose**

The purpose of this thesis is to contribute to research studies for lowering the costs of components using PBF-LB. The research focuses on the way printing parameters are affected along the process. This report intends to prove that PBF-LB can be used for mass production and that industrialization constitutes the next step of this technology.

### **1.4 Aim**

The objective of this master thesis project is to generate a gas manifold design for high build rates based on AM advantages. Specifically, a manifold is to be designed for PBF-LB with printing parameters guiding the design freedom. Quintus Technologies, being in the same field, has an idea of implementing the component into their system. This can serve as a practical example of how much the AM design can affect the part and the process. The goal is to streamline the printing process, optimize material utilization, and shorten production lead times, which simultaneously reduce costs and maintain high levels of performance of the components.

### **1.5 Scope of the thesis**

Within this master's thesis, the primary focus is to explore the potential factors that can enhance productivity in components fabricated using PBF-LB technology. The research scope includes a comprehensive literature review that examines relevant studies and methodologies associated with addressing various types of defects and defect modes in PBF-LB processes where Nitrogen gas can be employed as the processing gas during the printing process. This literature review provides a foundation for understanding the current state of research and techniques in the field, serving as a basis for the subsequent investigation into effective parameters for improving productivity.

Furthermore, the scope is limited to designing components for PBF-LB and the project contains no experimental tests but focuses on theoretical modeling techniques as the simulations are more time efficient.

### **1.6 Research questions**

This subsection outlines the key questions that the thesis project aims to answer. The research questions are specific, measurable, and relevant to the research objectives.

Research Question 1: What are the relevant parameters for design of a gas manifold to improve functionality using advantages of PBF-LB?

Research Question 2: How to design a gas manifold for PBF-LB to improve functionality, minimize pressure drop and decrease support structures while printing?

### **1.7 Report outline**

The thesis report aims to provide an understandable overview of the structure and composition of the research document. It outlines the main sections and subsections, giving the reader a clear understanding of the content and flow of information. The outline, in the index page, provides a structured framework, beginning with the literature research and explanation of the technology, leading to the project setup, and concluding with the results and future developments in the field.

# 2

## Theory and Literature Review

*This chapter describes technology in detail with the supporting research that has been done previously, by studying the literature and addressing the technological components and processes intensively including the research gap. The outline for this chapter delves into AM, specifically PBF-LB, HIP and its advantages along with the challenges.*

### 2.1 Additive manufacturing

Certain aspects of Additive Manufacturing (AM) are linked to complex design structures, adding advantages in terms of product usage or lifecycle or reliability, when compared to the conventional manufacturing methods. According to ISO/ASTM 52900 terminology, AM is the process involving materials that are bonded layer upon layer in order to create parts based on 3D model data. The main principle related to the technology is that Computer Aided-Design is used to define the geometry of a product that needs to be printed and then the 3D-printer builds the product layer by layer utilizing one or a mix of materials. By depositing or curing materials incrementally, AM enables the creation of complex geometries, customized designs, and lightweight structures. For example, nowadays, researchers are investigating the potential of AM to facilitate the supply system generating easily and quickly spare parts in aerospace industry [13]. With its potential to revolutionize various industries, AM stands as a disruptive technology with a promising future.

#### 2.1.1 Powder Bed Fusion – Laser Beam

One of the most mature and industrially utilized AM technologies is Powder bed fusion–laser beam (PBF-LB). It is a technology that is used by many companies as their main manufacturing method. It has a good potential to enhance the attractive aspect in this technology and the reason is its many advantages [14]. In contrast to other AM technologies, PBF-LB processes offer the opportunity of generating metal parts with a complex geometry without tooling or castings [15]. This can help to integrate many components into one and decrease the overall printing time [12]. This is impossible to do using a conventional method. It is a technology where melting and solidification occur in many areas at the same time, and this is because of the ability to control the laser power or the number of laser beams [16]. This contributes to decreasing printing time and, in turn, enabling bulk production. Moreover, the broad field of materials that can be used in PBF-LB [17] makes it

even more suitable candidate for many industries. This wide freedom of choice enables engineers to create components of customized features and better properties. Finally, another advantage of the specific technology is the material utilization and the essentially low material amounts that are wasted. To be more specific, after the printing process, the powder is reused [18] leading to less material consumption compared to other manufacturing processes and this is important when it comes to mass production where material is used to a high extent.

PBF-LB is characterized mostly by the laser beam that is used to melt and fuse layer-by-layer of powder shaping the final product. It is a modernized version of a process named “Selective Laser Sintering” and the main variation is that the new version enables users to generate metal parts or tooling of high density [14].

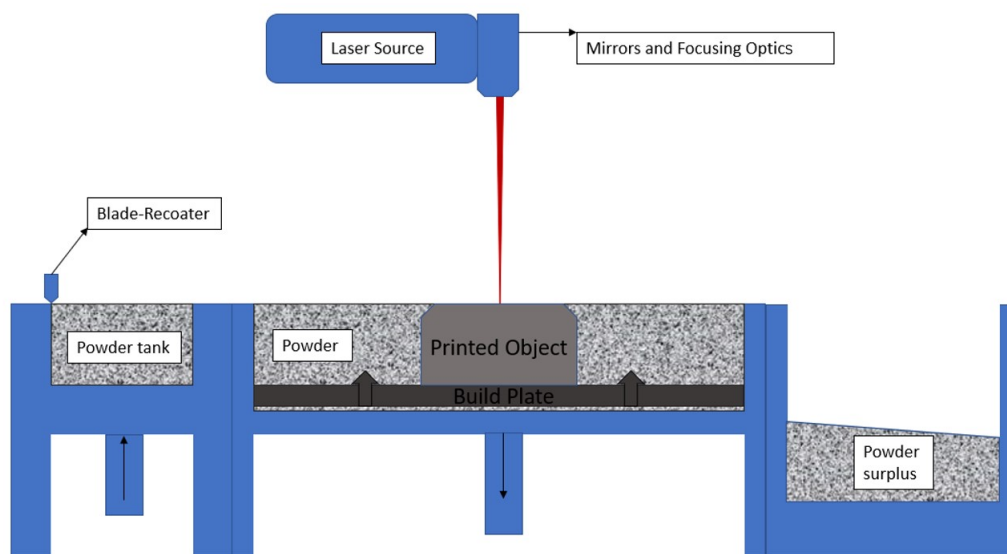


**Figure 1:** Schematic representation of the PBF-LB Process inspired by [19]

As it is presented in the schematic in Fig.1, PBF-LB consists of several key parts that work together to create complex and precise metal components [20]. The process and those parts are described as follows.

Firstly, a powder delivery system which includes a recoater such as a blade or roller applies a layer of powder in the central tank on the build plate [21]. Then, the laser source generates the beam which through mirrors and focusing optics selectively melts and fuses the powder grains based on the CAD geometry that is given to the system [22]. The laser scan speed and other parameters are regulated by the printer user. Depending on the layer thickness that is decided, the build plate is moving downwards and then the process is repeated again with the application of a new layer of powder. In every cycle, one new layer of the work piece is generated and the cycles are repeated until the whole printing process is completed. The distance range that the platform travels in every printing loop varies from 20 to 100  $\mu\text{m}$  [21]. In Fig.1, the existence of one more tank with powder can be easily observed on the right side of the central one. This is used as a powder deposition tank since in each

cycle, powder that is not thermally treated or used is saved in this collector bin by the recoater.

During the process, inert gas namely, nitrogen or argon is used to prevent the powder or the printed object from oxidization [22]. In addition to this, it facilitates the removal of condensate that occurs during melting and, in general, it affects positively the quality of the printed products [22]. Also, monitoring systems play a significant role during the PBF-LB process due to its intense conditions [23]. Surface quality, mechanical properties, and accuracy are controlled or optimized because of the fact that sensors are used and offer useful data which in combination with other information can contribute to the enhancement of the result [24]. The sensors collect information related to the temperature, melt pool, powder emissions, vibration, etc. [23].

This particular AM technology enables complex metal parts to be manufactured with high quality. This layer-by-layer approach controlled by selective laser melting enables production of complex geometries that would be challenging or not feasible using traditional manufacturing methods. The process offers the use of a wide range of materials and the printed parts have mechanical properties that can be compared to parts manufactured with conventional methods [25].

### **2.1.2 Design Process for AM**

The design process for components specific to PBF-LB involves several key steps to ensure successful printing [26] and this thesis report sheds light on designing a 3D-printed gas manifold that will replace old ones manufactured with conventional technologies.

Regarding the procedure, first come the design considerations and understanding of the capabilities and limitations of PBF-LB which is crucial [21] at the initial stage. Specific design guidelines for PBF-LB provided by device manufacturers or industry standards should be followed. These include support structures and additional features which are to be modelled in CAD software like Catia and Autodesk Fusion 360. Utilizing CAD software, the component's digital model is created. Regarding the design, the desired function, structural requirements, and specific considerations related to PBF-LB like the overhang angle and support structures as planned in the initial stage should be taken into account. As for the overhangs, they are created when the angle range between the printing object and the base plate varies from  $0^\circ$  to  $45^\circ$  [21]. They can cause severe problems such as distortion or warping which can lead to failure [21]. The support structures contribute to material consumption and influence the part in both negative and positive ways. Hence, determining the optimal alignment of parts within the build chamber is critical and it is complicated to achieve desired mechanical properties and minimize post-processing efforts [27]. Support structures are intended to provide stability during printing and are usually generated automatically by particular software. Optimization of the support struc-

ture reduces material consumption and post-processing effort. The digital model must be in a format compatible with the PBF-LB.

The developed 3D model is imported to simulation software like Materialise Magics to understand how support is generated and get an idea of orientation. Also, using the particular printing parameters in the process, as the part is supposed to be printed with. After that, the part is subjected to simulation for potential issues like distortion.

When the final design is ready, the printing process is started in the machine and then the required post-processing procedures are followed. Heat treatment, hot isostatic pressing, surface finishing, machining, laser peening are some of them [28]. Support removal is also a post-processing procedure but it is intended to reduce in this project.

### 2.1.3 Materials in PBF-LB and 316L Stainless Steel

The selection of materials for PBF-LB depends on variables such as the required properties of the ultimate component, and its application. Some material groups from the wide range of options include metals, polymers, and ceramics. The technology is utilized to print a range of metals and alloys such as stainless steels (SS), aluminium-, titanium- and nickel-alloys, etc. [29]. Also, polymer materials like nylon belonging to the thermoplastics group, polypropylene, and polyetheretherketone can be utilized [22] and, finally, in spite of the fact that it requires a different procedure, ceramic powders including alumina, zirconia, and silicon carbide, can be used in PBF-LB [30].

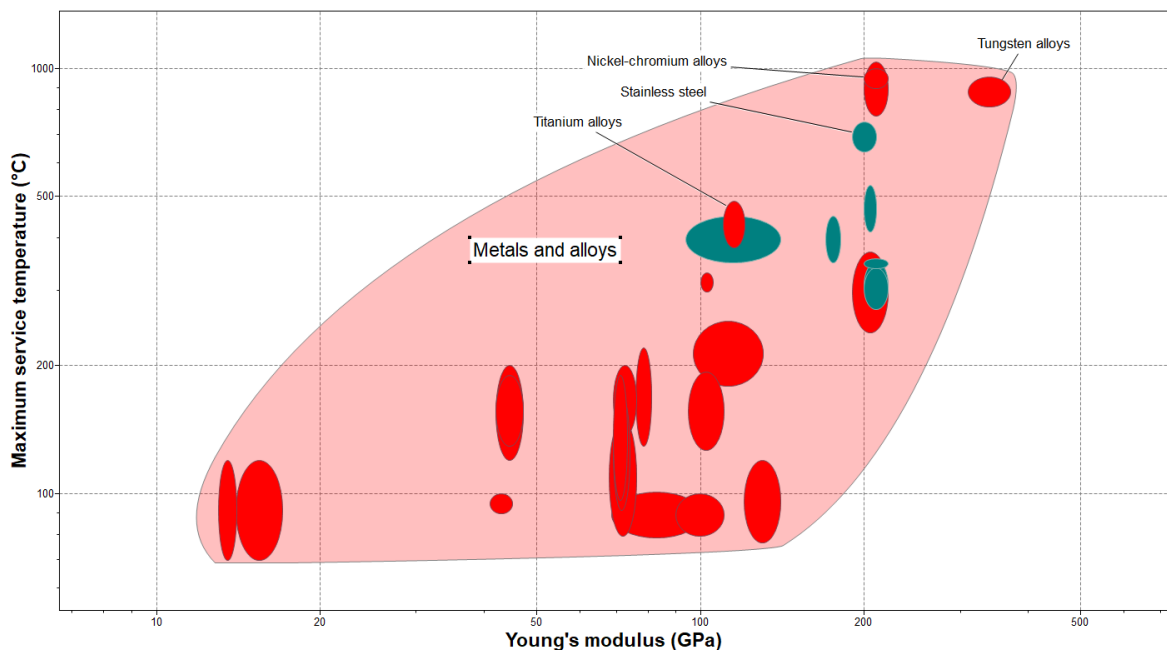


**Figure 2:** Maximum service temperature vs Young's modulus graph

The trend of strength and maximum service temperature for metals and alloys is shown in Fig.2, made in Granta Edupack. Ceramics and Polymers are not included in this analysis as the scope is directed more to metal powders. All the highlighted materials are in the usable list for PBF-LB. But in this thesis, SS 316L is considered from the range of materials, as the application range for this material is wide and it is compatible for printing in argon or nitrogen atmosphere. Also, this is the most used material for the intended application - gas manifold.

Here, in the Fig 2, 316L can be seen as optimally good for components common applications like in industries typically focused on food processing, nuclear, corrosion environments, petrochemical and off-shore sectors, in terms of strength, manufacturability and cost.

The combination of SS and PBF-LB is widely used as it has many applications from household products to industrial equipment [31]. Quintus Technologies equipment consists of parts made of 316L stainless steel and components include manifolds and hydraulic blocks similar to the component designed in this work.

### 2.1.4 Advantages and Limitations

Over the years, significant development has been made in the PBF-LB process. Key improvements include the implementation of gas flow control, the integration of multiple lasers, and the usage of advanced sensors. These advancements have led to rapid enhancements in both the process quality and the manufactured products. Especially, the uniform inert gas flow plays a vital role since it stabilizes the process of fusion during the PBF-LB process and, simultaneously, dimensional variations tend to decrease [15]. Also, many improvements contributed to lead-time reduction. Powder management technologies have been developed and succeeded in eliminating the time-consuming installation procedure [32] while multi-lasers enable fusion in many points on the bed at the same time making the procedure quicker.

On the other hand, PBF-LB main disadvantage is that it can sometimes be expensive to print and build rates remain very low [29]. To be conducted properly, the specific technology requires fine layer thickness and hatch space, factors that contribute to decreasing production time [15]. In addition to this, surface quality of printed components can be a challenge, a fact that can lead to additional post-processing, and, in turn, prolonging the product development lead time. For the cases where the build rates are increased, the parts are induced with abnormal features. [33]. Porosity is at the top of the list [34]. Researchers have proven that developing and implementing thicker layers can speed up the printing process as the number of layers in the overall component that needs to be printed are reduced. This leading to slightly more porosity [8].

### 2.1.5 Porosity effects on AM component

Pore defects are commonly observed when PBF-LB is used for manufacturing. Lack of Fusion (LoF) and gas porosity are the most common ones. X-ray imaging and numerical models have been employed by researchers to investigate how porosity originates. Researchers have looked into a variety of methods to control them including modifying the powder feedstock or adjusting process parameters [34].

LoF is a type of defects that is more process controlled. Modifying the parameter set such as the scan speed, laser power, scan track will affect the occurrence of this porosity. LoF occurs when molten powder is not completely fused with the lower layers in the printing process. This results in some unfused regions. These regions affect the part in a negative way, as the mechanical properties are affected negatively and tend to fail more rapidly due to stress concentrations and crack initiation points than the rest of the regions. Therefore, it is important to control and eliminate LoF consequences during PBF-LB processing. Hence the final products are desired to have no to very little porosity for the above reason. These pores are longer and sharper than other pore defects [35].

Another type of pore defect is known as gas porosity. There are two categories of gas porosity, such as keyhole porosity and starting powder porosity. The gas porosity is when gas is trapped during the melting and solidification process at the time of printing [36]. This process is very common for occurrence of keyhole pores, which are typically spherical and their size is small [37]. For the other category, the gas is already induced in the powder bed and chamber even before start of the process and released when the powder is melted [34]. This can be a result of the powder itself, depending on the manufacturing technique or storage. All these porosity types hugely effect the component's performance.

### 2.1.6 Recoating time

Recoating time is also a factor that contributes to printing part build time increase. Layer thickness, powder size, powder shape, and recoater blade shape are some of the parameters that can influence recoating time [38]. Apart from the printing time, powder layer density and surface quality are also affected by how quickly the recoater moves during the AM process. Despite being a potential factor, it is impossible to avoid or reduce drastically the recoating time, productivity of AM is affected very little at this point of time.

## 2.2 Hot Isostatic Pressing

HIP is a post-processing technique commonly used in AM that can improve the mechanical properties of 3D printed metal components, by healing the defects occurred during the printing stage as discussed in [39]. However, HIP can also introduce expected yet undesirable outcomes into the printed part, adversely affecting

the component like grain coarsening and change in microstructure.

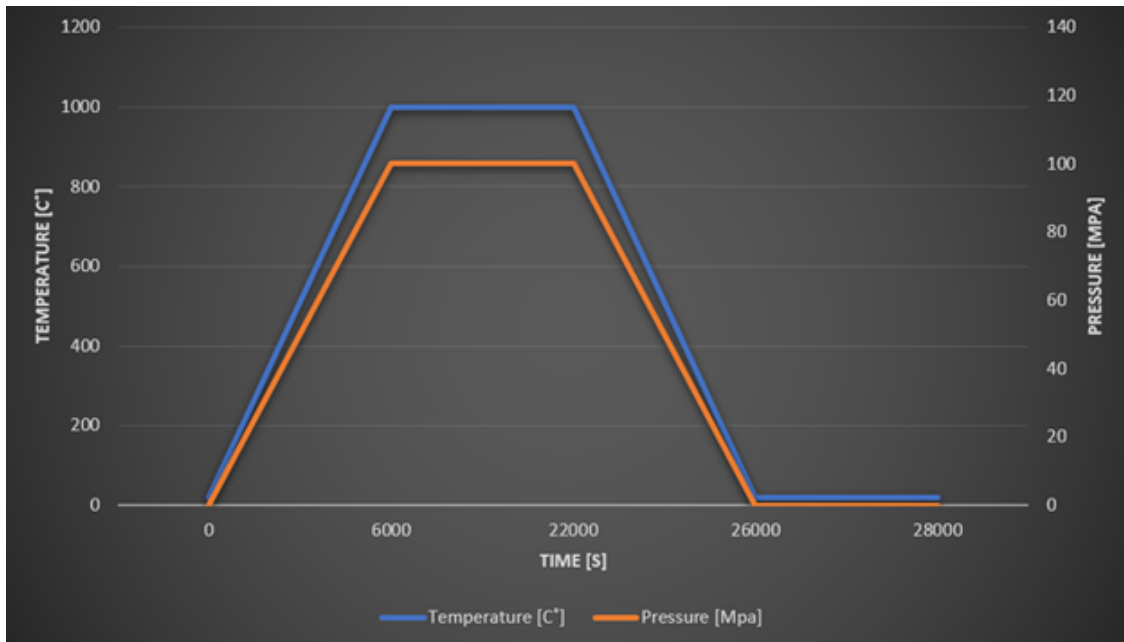


**Figure 3:** HIP Cycle Graph

The process can be characterized as the exposure of a component or metal powder to a combination of high temperature and extreme pressures for a certain period of time. A notable feature of this is the usage of a gas that plays an essential role in increasing the pressure of the system. Since the process includes the word “isostatic”, the same amount of pressure is applied on every side or surface of the exposed object including the channels. The main gas that is commonly used nowadays is Argon. Besides, Nitrogen is used in some cases for specific materials such as ceramics. A typical HIP cycle is presented in Fig.3. These parameters are different from those used in this thesis project.

The Fig.3 is inspired from [40]. This is an example of what happens during HIP in terms of time, temperature, and pressure. The object destined to go through this process, is heated from room temperature to elevated temperatures. At the same time, the pressure starts to rise in a similar way as the temperature reaching the required number. The object is exposed to both high temperature and pressure a pre-determined length of time when, suddenly, the cooling process and decompression are activated. Being a heat-treatment process, the microstructure of the exposed part is affected and as the component will be in a plastic state, the component tends to be fully dense by healing the formed pores during the printing stage.

The equipment for HIP consists of a furnace, a pressure vessel, a gas-handling system, a control system, and auxiliary systems [39]. The pressure vessel is an important component since it includes the furnace which keeps the temperature at high levels while, at the same time, it maintains the gas in high pressure. The role

of the furnace is obvious, and this is providing the HIP system with heat. The heat is transferred mainly with convection phenomenon between heaters and the component while the gas acting as the medium [39]. But also, radiation starts to contribute while in high temperatures [39]. A Gas-handling system is necessary since, as it was mentioned in previous paragraphs, argon is used for surrounding the exposed object with pressure and as a heat transfer medium between the heaters and the components being subjected to HIP. A micro-computer or a programmable controller can be the control system of the process which is responsible for making the whole HIP cycle automatic [39]. The auxiliary systems consist of the cooling, material handling, and vacuum system [39]. The cooling system plays an important role in setting boundaries and controlling the system's pressure.

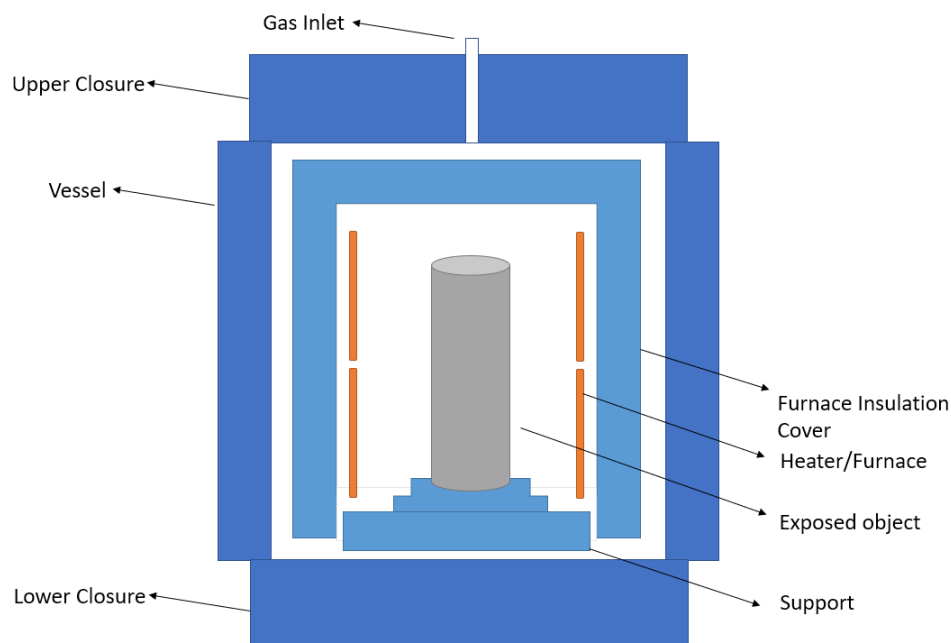


**Figure 4:** Schematic figure of the Hot Isostatic Pressing process

The schematic in Fig.4 represents in a simple way HIP equipment. This schematic, which is inspired by [41], constitutes a simple version of presenting what HIP equipment consists of. As the image depicts, the object is placed in the hot zone being surrounded by the vessel, lower, and upper closure. The gas which is responsible for increasing the pressure of the system enters the facility through a small inlet located in the upper closure as in the Fig.4. But the Quintus equipment uses the bottom closure as an inlet for gas. Inside the pressure vessel, there are also more parts that surround the workpiece. Firstly, the support where the object is placed on and the furnace insulation cover. Secondly, the furnace heaters are placed closer to the exposed object as a way to offer heat to the system. Typically, pressures that are used in these systems are up to 200 MPa while temperatures do not exceed 1400C for metallic materials. Generally, temperature reaches approximately 80% of the materials melting point, but there are exceptions for some materials like Titanium

[42].

In powder metallurgy, the Hot Isostatic Process has been industrially being used since 70s. This process has great importance in producing high quality billets and components in terms of mechanical properties including density and ductility [43]. In modern industries, it is mainly applied for sintering of specific steels, healing of superalloy and titanium castings, as well as post densification of cemented carbides [44].

In AM, HIP can be used to heal defects after the print which increases the structural integrity of printed components. HIP can be done as post processing procedure for AM technologies like PBF-LB and Binder Jetting. Also, metallic or non-metallic materials can be used for this process. For commercial production, the high-resolution printing capability of PBF-LB and Near Net Shape capability of HIP forms as an effective complete process, eliminating the need for longer logistics duration, adding to the cost reduction [45]. Although there are many key parameters that can be adjusted for the appropriate results in HIP stage like the temperature, holding time of the gas used, there are still indefinite effects, mainly, the shrinkage that needs to be addressed for maximizing the mass production.

### 2.2.1 Simulation of Hot Isostatic Pressing

The plasticity influence was studied in [46] on the final geometry of post-HIP components in their FEM program, Abaqus, for “near-net-shape” simulation. They used Abouaf’s [43] creep model, one of the widely used numerical model in this research area and improved it for temperatures and pressures that vary. The combined model showed good prediction of the initial creep and was found to be better than other models in showing how the component transforms physically during the HIP process. The study suggests creation of optimally ranged wall thickness of component capsules. This range aims to minimize the need for post-process machining and reduce waste material.

Another research [47] focused on the simulation and optimization of the HIP process for metal components. The authors utilized finite element analysis to investigate various aspects of the HIP process. Although, this work considered titanium components, it examines more on the design of the capsule. The former paper gives an idea on the process variables for instance, temperature, pressure, and time, on the densification behavior of metal powders during HIP. Both studies provide valuable insights into the optimization of the printing process, aiming to improve the quality and performance of the final components.

By leveraging finite element simulation, these studies contribute to advancing the understanding and optimization of the HIP process in the production of metal components. These simulations give an advantage to be very effective in terms of resource usage, like reducing the duration it takes to print and test by a large margin.



# 3

## Methodology

*This section of the report includes a clear and detailed description of the methods and procedures used in the study, research design, and any limitations or assumptions that affected the validity and reliability of the results.*

### 3.1 Research Design

The flow chart below explains the anticipated process according to the research.

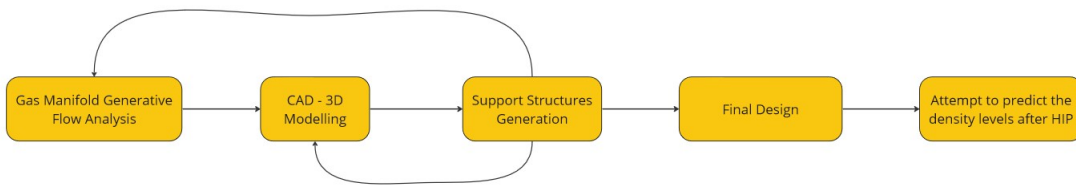


**Figure 5:** Process Framework

As the goal of the project is the development of a gas manifold for AM, the research begins with a Generative flow analysis aimed at optimizing the flow in the gas manifold based on fluid dynamics principles. This analysis helps determine the efficient design of the gas manifold, given the design space.

Once the flow analysis is complete, a CAD software namely, Autodesk Fusion 360 is used to design an initial gas manifold design by 3D modelling techniques. The support structures required for the AM process are generated by Materialize Magics software. The design goes through multiple iterations and refinements based on feedback and evaluation from the results of previous iterations. These iterations help improve the performance and functionality of the design.

As the final design is made, an attempt is made to predict the densification levels after HIP was performed. Multiple densification levels are simulated to understand the process better. Throughout this work, SS 316L was the material of choice for the component as discussed in section for materials (see Subsection 2.1.3 ).

The research project anticipates the process led to the systematic design and optimization of components for AM, considering factors such as flow optimization, support structure generation, and prediction of densification levels using porosity levels during the HIP process.

### 3.2 Generative Flow Analysis

To optimize the design of the gas manifold for PBF-LB, fluid dynamics of the gas used in the application needed further clarification. To achieve this, a Generative Flow Analysis (GFA) was performed. GFA involves creating a digital block model of the manifold (Fig.6) and simulating gas flow through the manifold under various conditions. This includes different pressure levels, inlets and outlets which provide essential input connected to the manifold design requirements and how they can be improved to optimize gas flow in case of the component produced by additive manufacturing.

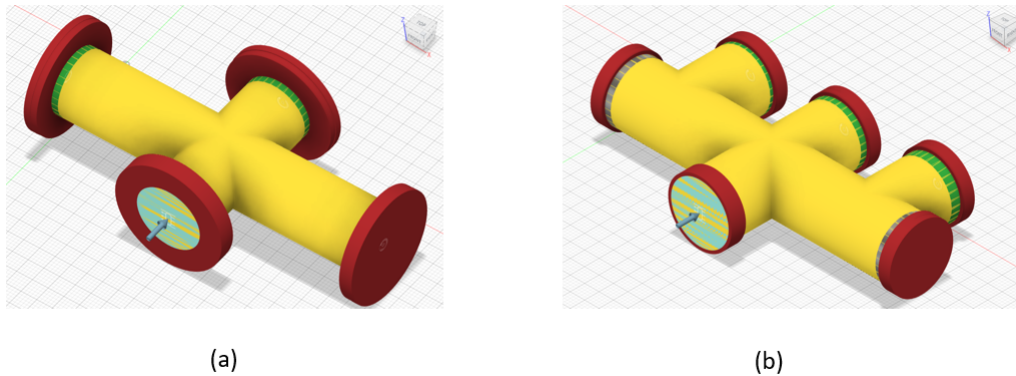


**Figure 6:** Generative Flow Analysis (a) Block model Version 1 isometric view (b) Block model Version 2 isometric view

GFA was performed iteratively to adjust the manifold design based on data given from the design team at Quintus, see table 1.

As the input data was limited, there was a lot for design space and exploration. Other than those, some of the specifications are assumed to suit the simulations.

**Table 1:** Requirement list for manifold

Requirement	Figure
Inlet and Outlet size	15 – 20mm
Max capacity	
- Continuous flow:	25MPa
- Maximum point:	30MPa

One of those was a fixed magnitude on the flow rate as 7.5 liters per minute and the other is the percentage of design volume. The latter parameter can be varied depending on the experimentation, and the difference can be seen when there is prototyping stage. As this project does not include any model prototyping, the design volume is defined with only one value, which is 25%. The material optimization percentage is set to that value ensuring that there is not much material put on the part and at the same time it is not very little for the part to cause failure. The objective when starting the simulation in the dialog box was set for minimizing pressure drop.

As a new feature in the software, it was only able to solve the simulation for minimizing the pressure drop, which works for the design because it is one of the attributes for a good manifold design.

This iterative process allowed for a more focused and efficient approach to designing AM manifolds, as the results of each simulation could be used to improve the design of the next iteration. In the context of AM, the unique requirements of the process should be taken into consideration, which specify a special design approach. This includes factors such as the orientation of the part during printing, the flow of material, and the distribution of material within the part. These considerations are essential in achieving optimal results for obtaining the desired quality and functionality of the manufactured components. By running the flow analysis, the development of a manifold design specifically optimized for the AM process was made possible, resulting in increased efficiency and performance, optimizing the material used.

As in the Fig.6, the blocks of the manifold designs are to be fixed with some constraints represented by different colors. These constraints are presented in table 2, showing them in detail. To achieve the desired final component, it is important to ensure that the gas flow is optimized, and the manifold design plays a crucial role in this. Ensuring optimized gas flow is critical to achieve the desired final component, and this can only be done at manifold design stage.

**Table 2:** Constraint codes for colors

<b>Color</b>	<b>Constraint details</b>
Red	Obstacle Geometry
Green	Flow Source and Openings
Yellow	Starting shape for fluid

By analyzing the results of these simulations, we can gain insight into gas behavior and identify design improvements that could improve manifold performance. This ensures that the gas flow is directed in the desired direction that the pressure and heat have optimal impact on the printed component. As seen in the Table2, the inlet and outlet ports are shown in green as they are critical points for gas flow into and out of the manifold. The obstacle geometry is created as the boundaries for flow analysis where needed. In the middle of the constraints there will be a starting shape of the fluid to follow when the analysis is started and then the com-

puting is done as the first step. By simulating gas flow behavior using GFA, designs that consistently and efficiently affect the production rate, yielding high-quality end products are developed.

## 3.3 Design for AM

Relied on GFA, a design approach for AM followed. Autodesk 360 Fusion being the main CAD tool of the research facilitated the process of giving shape to the project's manifold. Because of the fact that high productivity was the goal, a challenge that needed to be resolved during the research was how to arrange support.

Thus, the process involved testing the component in several orientations to determine which is best suitable using Materialise Magics, a software program specialized in data and build preparation for AM. Also, replacing the support structures with material and adjusting the angles of support-needed features played a significant role. All these steps were repeated a lot of times in order to finalize the design.

## 3.4 Simulations

The manifold's design completion paved the way for an attempt to predict how densification behaves in a component after HIP. Previous studies related to density levels estimation [40], have utilized programming or the Ansys software for prediction. Due to limitations in scope and time, a different approach was chosen within the frame of this study. The simulation of printing and HIP was performed using the Simufact Additive software.

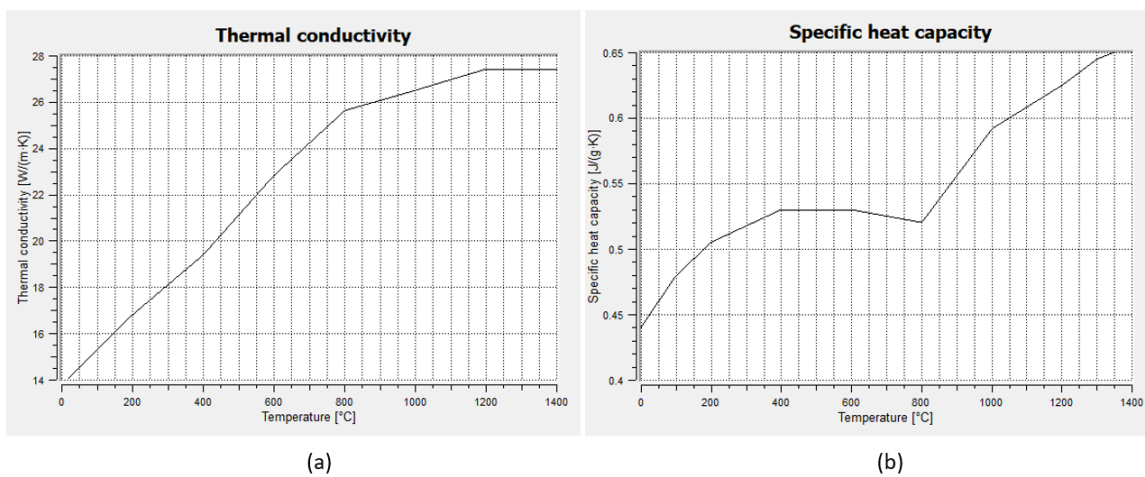
Simufact Additive is based on the MSC Marc software algorithm and offers the opportunity to evaluate different manufacturing steps connected to Additive Manufacturing and it enables users to predict material properties that occur after HIP as well. The manufacturing steps simulated in Simufact were printing, cutting, support removal and HIP. Cutting is defined as the phase where the support structure that bonds the component with the baseplate is being cut so that the printed part is detached.

Thermal conductivity data, specific heat capacity data and composition information were collected from Simufact Additive Materials Library. The chemical composition can be seen in Table 3 Regarding the HIP process and densification calculation, the corresponding parameters are presented in Tables 4 and 5. The information regarded the densification parameters were inferred from [48] and they are about the austenitic stainless steel 316L.

Since the intended material for the Quintus manifold was 316L stainless steel its thermal material properties were used for the simulations. The graphs in Fig.7

**Table 3:** Composition of SS 316L

<i>Element</i>	Percentage mass portion
C	0.009
Cr	16.82
Cu	0.31
Mn	1.74
Mo	2.08
N	0.029
Ni	10.26
P	0.03
S	0.024
Si	0.27

**Figure 7:** Thermal Properties for SS 316L (a) Thermal Conductivity/Temperature (b) Specific heat capacity/Temperature

present how thermal conductivity and specific heat capacity change dependent on temperature.

**Table 5:** Densification Calculation Parameters

Temperature (°C)	Yield Stress (MPa)
20 (Room Temperature)	200
1060	30

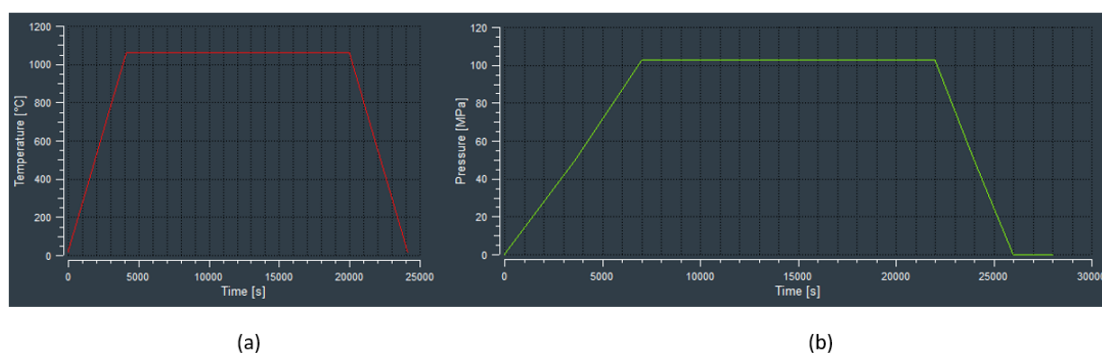
The previous tables include numbers that are similar to the HIP process conducted for research of Oregon State University [40]. This is because the goal was to compare and validate the results. In this similar project, Ansys software was used in order to predict the densification levels that the exposed component reach after HIP process in contrast to this thesis where Simufact Additive is the simulation tool.

As shown in Fig.8, these are the HIP parameters used in the simulation presented

**Table 4:** HIP Parameters

Parameter	Value
Initial Temperature	20°C
Temperature Ramp Rate	0.25 K/s
Maximum Temperature	1060°C
Temperature Holding Time	4.4 h

as Temperature/Time and Pressure/Time graphs. The simulations were conducted for both gas manifold and simpler geometries such as cylinders of different sizes to comprehend how the model reacts and what results it generates.

**Figure 8:** (a) Temperature Time Graph (b) Pressure Time Graph

### 3.4.1 Challenges during simulations

In the context of simulations and calculations, the trade-off between accuracy and computational time is very often. Achieving higher accuracy in simulations typically requires more computational resources and longer computation times. On the other hand, reducing computation time often involves simplifications or approximations that may affect the accuracy of the results.

While using the software, we dealt with several calculating errors. These errors occurred only during the HIP process and one of the main reasons was the fine meshing grid. Simulations were conducted in different kind of element sizes but there was a boundary. When a meshing size below 1.5 mm was chosen, then software could not generate results.

## 3.5 Different Porosity Levels

Even though porosity is an unwanted phenomenon, there are scenarios where engineers intentionally manipulate and control porosity to their advantage. One of the benefits of controlling porosity percentage is the reduction in component weight [31]. By strategically incorporating porosity into the design, the overall weight of

the component can be decreased without compromising its structural integrity. In this case, HIP is not used since it adversely affects the structure. Furthermore, intentionally introducing controlled porosity can also lead to increased productivity in AM [49]. Porous structures can be fabricated more quickly compared to fully dense component since the presence of voids allows for faster laser scanning and decreased energy requirements during the printing process. This can result in shorter production times and improved efficiency. When it is combined with HIP, the opportunity of having dense parts in a quicker way is offered. To statistically process how much this parameter affects the build rates the simulations are to be tested by physical experimentation and validate the numbers. Something that should be mentioned is that the extent and distribution of porosity should be carefully controlled and optimized to ensure that the desired trade-off between weight reduction, productivity, and mechanical performance is achieved and aiming to maximize the benefits while minimizing the potential drawbacks associated with porous structures.

The thesis project includes calculations and attempts to predict the relative density that occurs in a component after HIP. Multiple density levels are considered and the highlighted observations are shown in the following sections.



# 4

## Results and Discussion

*This chapter includes the findings of the thesis that are objectively presented and discussed in detail.*

### 4.1 Preliminary Design

Based on the parameters outlined in the methodology (Chapter 3), the design process was implemented to obtain the results that will be discussed in the following sections that can be printed using PBF-LB. The iterative design process involved several key adjustments from the steps discussed below.

#### 4.1.1 Manifold Design - Generative Flow Analysis 1

When the pre-processing requirements are fulfilled, the status in the ribbon tab of the software is turned to a green tick indicating that the simulation can be started. The simulation time of these components was approximately twenty minutes. The design iterations were then separately compared in the first iteration, with two inputs. One has one inlet and 3 outlets, and the other model was run with an equal number of inlets and outlets as model outputs below.

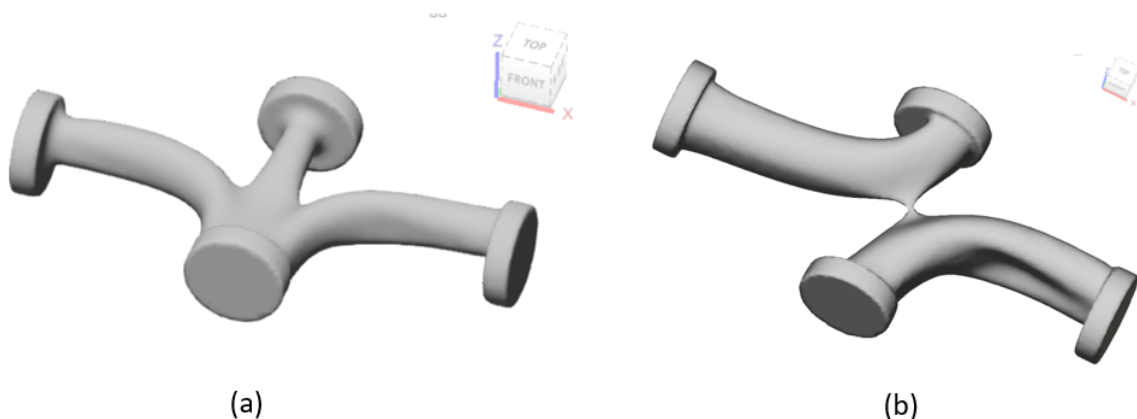


**Figure 9:** GFA-1 Models (a) Model 1 (b) Model 2

As model 2 (see Fig.9b) yielded two separate channels, it did not satisfy design requirements and was hence not considered. Following the design process for AM,

there were mandatory design changes needed to be implemented which led to a different block design for the GFA. As the design was protruding outwards at an angle of  $90^\circ$ , it was impossible to print the component without support structures. Support structures require additional post processing steps which makes the component more expensive. Therefore, further design iterations were performed with emphasis on lowering the build angle to prevent the use of supports. The simulation procedure was repeated with a focus on the number of inlets and outlets, with only 1 inlet and 3 outlets, resulting in the models that are discussed in results section.

The model was studied with the visual representation of its pressure reference and the flow magnitude also, in Fig10.

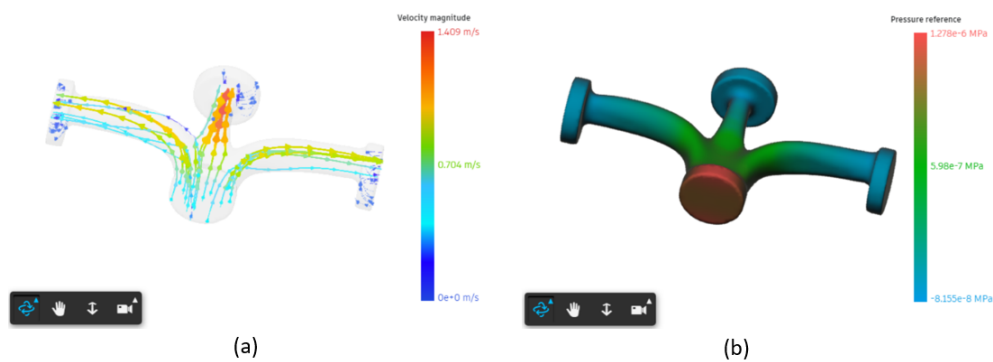


**Figure 10:** (a) Velocity Magnitude (b) Pressure Reference

### 4.1.2 CAD design

Based on the GFA, an initial manifold design was created that consisted of one inlet and three outlets, as illustrated in Fig.11.

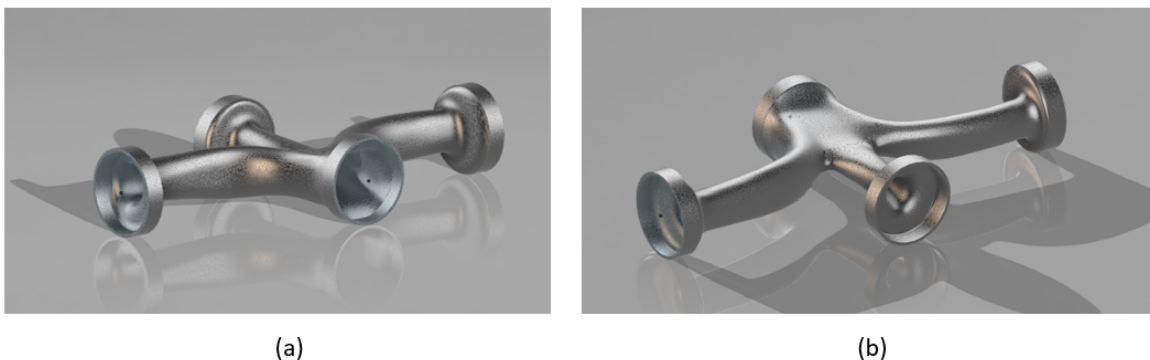


**Figure 11:** Manifold Design 1 (a) Rear view (b) Front view

The Materialise Magics software was used with a view to simulate the pre-processing stage in printing, that includes part orientation, support generation etc. The manifold was placed in different orientations and support generation was completed. As

the goal was to minimize the supports, possible orientations are analyzed to find out that all orientations are generating huge amounts of supports. All the orientations are presented in the Appendix B. As it can be easily observed, overhangs and angles that reach  $90^\circ$  contributed to creating a lot of support structures in each one of the tested orientations.

## 4.2 Iterations

Since the aim of the project was to minimize the need for the supports, the design was iterated focusing on the points where support is required. As one of the requirements, the design should be AM specific, and with an idea to simplify the piping layout, the GFA was done again, and the design was modified.

### 4.2.1 Manifold Design - Generative Flow Analysis 2

The understanding of how gas flows under given constraints is understood by the following results. The Fig.12 below shows the fluid flow model developed using GFA, considering the printability in AM.

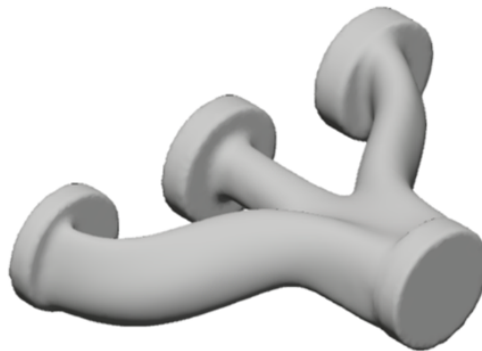


**Figure 12:** Final model of fluid flow

The first design was optimized to its best for reducing the pressure and material utilization, but for analyses purposes in project the second design is considered and it was exported into a CAD file and made into a manifold naming Manifold Design 1, which will be discussed further in the report. The Fig.13 shows the gas flow velocity magnitude and pressure distribution for the model obtained in GFA-2.

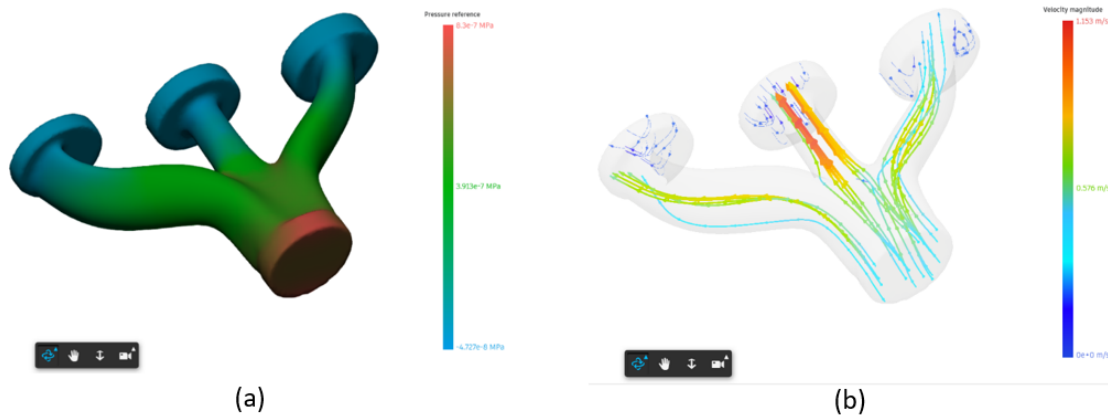


**Figure 13:** Final model flow analysis (a) Pressure reference (b) velocity magnitude

### 4.2.2 Comparison for GFA 1 and GFA 2

The comparison chart in Fig.14 provides a visual representation of the changes in key design parameters between the first and the revised manifold design.

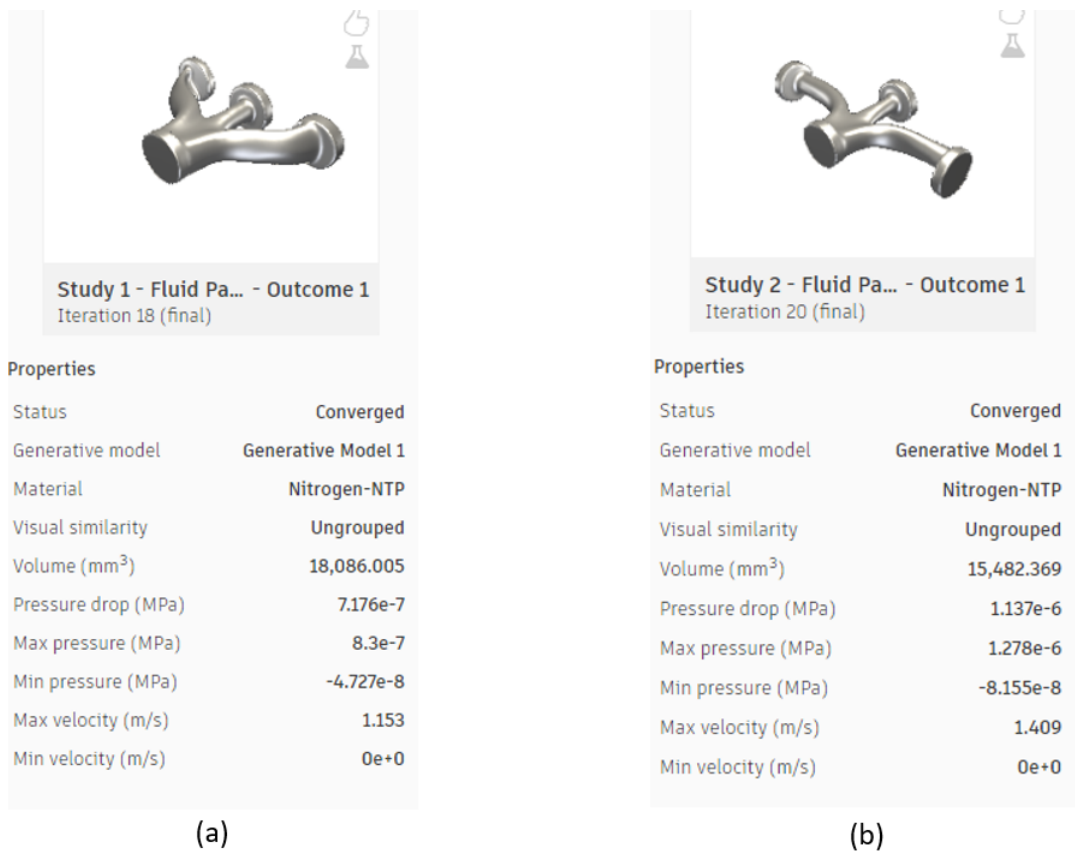


**Figure 14:** Specification comparison of GFA-1 and GFA-2

The chart shows a side-by-side comparison of the velocity magnitude, volume, and

pressure distribution for both designs. In the original manifold design, the velocity magnitude was higher in some areas, particularly in the inlet and outlet ports, resulting in uneven gas flow distribution throughout the manifold. The pressure and temperature distribution were also uneven, with some areas experiencing higher pressures and temperatures than others. This could potentially result in inconsistencies in the quality of the final printed component.

However, with the revised manifold design, the velocity magnitude is more uniform, and the gas flow distribution is improved throughout the manifold. The pressure and temperature distribution is also more uniform, resulting in more consistent heat and pressure distribution to the printed component. The pressure drop has been minimized by 51.5% from  $1.14 \times 10^{-6}$  to  $7.18 \times 10^{-7}$ . Overall, the comparison chart provides insights into the impact of design changes on key design parameters and their effect on the AM process.

### 4.2.3 CAD design

The CAD design after the GFA-2 is as presented in Fig.15, showing the changes incorporated for the benefit of design for AM.

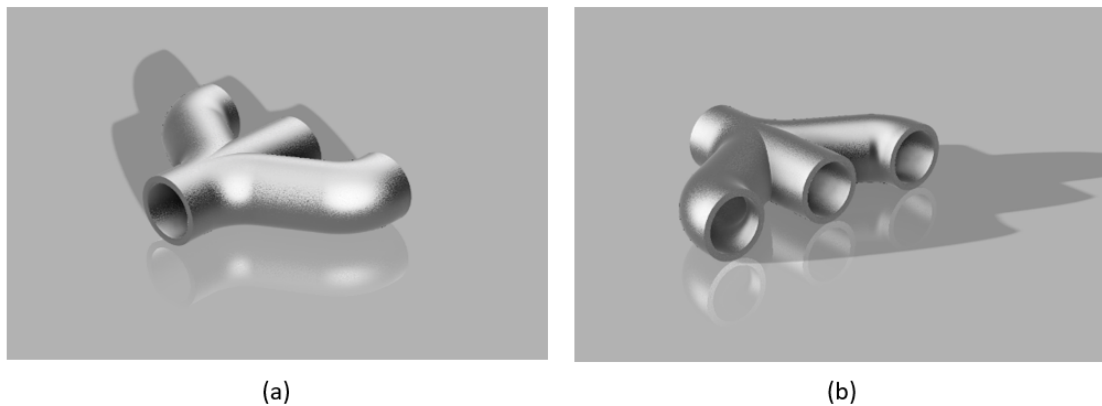


**Figure 15:** Manifold Design 2 (a) Rear View (b) Front View

Aiming for a more printable design, the direction of the flow paths changed while the overall width of the component decreased. The inner diameter of the flow paths was 16 mm and the thickness was 2 mm. However, the support structures could not be avoided again. Simulating the new design reduced the amount of supports needed but still some areas of the component required it. It was identified that some curves had concerning angles that might be hard to print. The orientations tested in this design iteration are presented in detailed in Appendix D.

In the case of applying the first, second, and third orientations (Appendix D a-f), the supports inside the paths cannot be avoided. Thus, these orientations were not taken into consideration for the rest of the research. Regarding the fourth (Appendix

D g,h) and the fifth orientation (Appendix D i and j), the latter was decided to be the perfect option. The fourth orientation was no longer considered as it would require more and higher support structures. As it was mentioned before, the design needed to be improved more extensively. It was decided that the orientation with the three outlets placed on the ground and the inlet pointing up (Appendix D i,j) was the proper one to move on for the printing process. In this orientation, the design can be modified in a way so that support structures are not needed.

### 4.2.4 Design 3

The results are presented in Fig.16.



**Figure 16:** Manifold Design 3 (a) Rear View (b) Front view

This design follows exactly the same pattern of one inlet and three outlets but smaller additional holes were designed intending to enable fasteners to connect the component to industrial equipment. The inner diameter remained the same but the thickness varies. Using again the Materialise Magics software, support structures seemed still to be unavoidable. (Fig.17).



**Figure 17:** Manifold Design 3 (a) Outer Supports (b) Inner Supports

Support structures are needed not only on the outer surface as it is seen in Fig.16a but also inside the manifold flow paths. The design changed again until the structures are eliminated. The differences and characteristics of each design are presented in the Appendix A.

### 4.3 Final Design - Analysis

After many changes and versions created during the 3D-modelling process, the last design of the gas manifold took its last form and is presented in Fig.18.

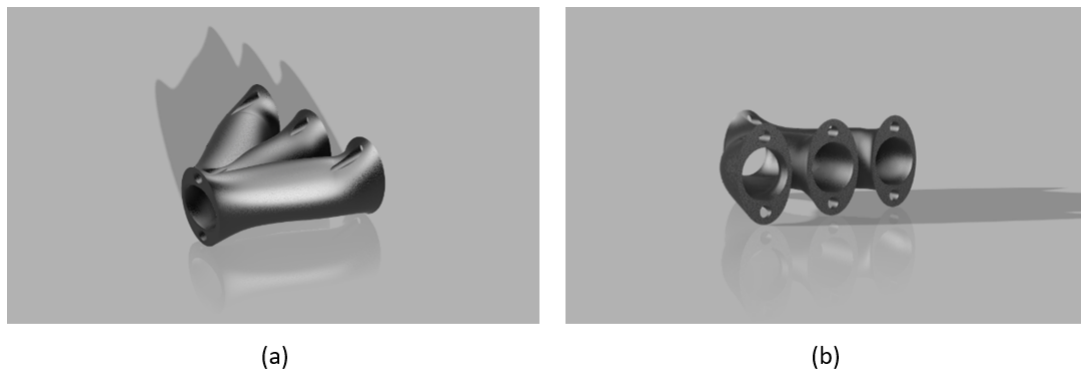


**Figure 18:** Manifold Design 4 (a) Rear View (b) Front view

The positions of the three outlets were placed closer to each other and more material was utilized in overall. The size of the component was reduced regarding the previous designs and the weight reached the 107.2 grams. As it is shown below, support structures are not needed in the final design.

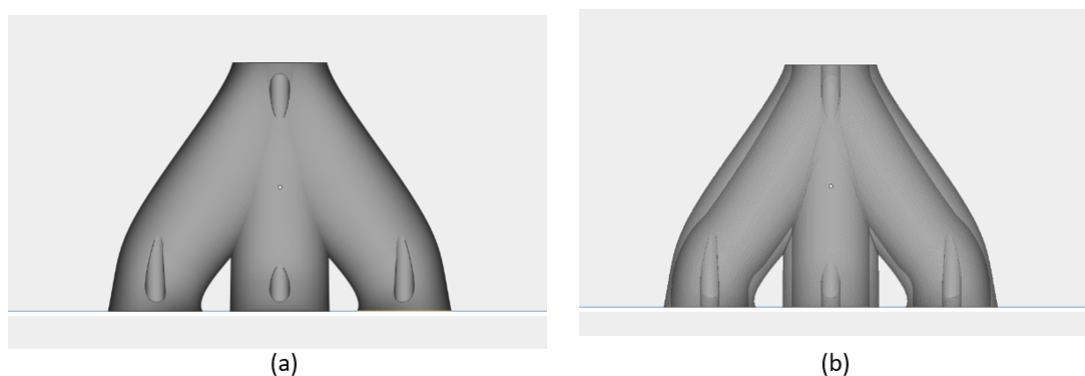


**Figure 19:** Manifold Design 4 (a) Solid view (b) Transparent view

In Fig.20, the progress of how the design changed through the project is presented.

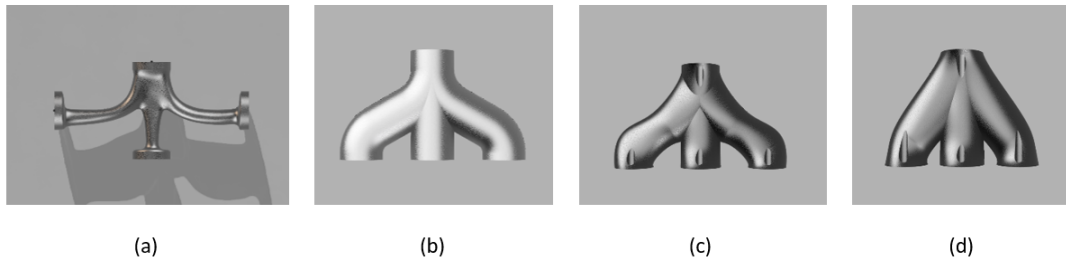


**Figure 20:** Design for AM Progress

The top views in Fig.20 show how the component was affected by the design for PBF-LB. Although the height is fixed, the width was adjusted according to the requirement of print ability in PBF-LB. AM is known about offering the opportunity for engineers to generate designs and components of high complexity. On the other hand, one should always design based on many parameters that are related to the printing process. In this thesis project, the goal was for the manifold to be supportless since high productivity and low production lead-time played a vital role. Support structures require additional post-process time since removal must be completed mostly in a manual way [27]. Also, they can degrade surface quality of the printed component leading to the need of a surface finish process. Thus, a large amount of material, energy, and time is demanded if supports exist in a design and because the focus of this research was on high productivity and mass production, a supportless design was decided to be created. Since this orientation (See Fig.20) had been decided as the most appropriate one, the manifold's features such as angles, dimensions, and flow paths directions were affected and altered.

## 4.4 Simulations

After successfully designing the manifold, an attempt has been made to simulate the HIP technique to collect relevant parameter information about the component densification. This is section about the results of those simulations, explained the process through out.

### 4.4.1 Simulations of HIP on gas manifold

As the purpose of this project was to assess the high productivity aspect using PBF-LB, designing a gas manifold and analyzing it using simulations is considered as a milestone in this process.

The 3D model of manifold was imported into Simufact Additive software. As discussed in the methodology, the simulation is carried out and obtained the following results represented in Fig.21.

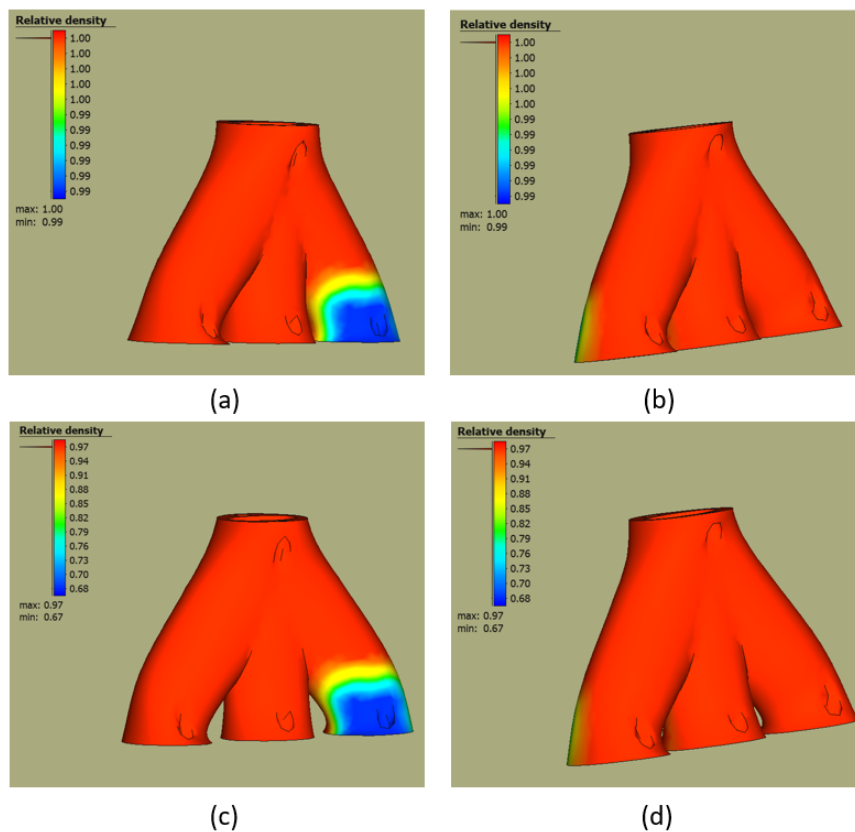


**Figure 21:** Manifold Simulations (a) 99% initial density, front view (b) 99% initial density, rear view (c) 67.5% initial density, front view (d) 67.5% initial density, rear view

Here, the gas manifold with an initial density of 99% was simulated, after HIP, the component is being densified up to 100%. It is to be noted that the relative density is uniform throughout the manifold, except for one spot. This abnormal variation covers a large part of the right side channel of manifold (See Fig.21a). In the case where an initial density of 67.5% was applied, relative density of the part reaches 97% but still a low density area is present in the same region (See Fig.21c), with slightly more variation in the abnormal dense region.

Attempts have been made to understand this abnormality, one of which is to consider a simpler geometry and repeat the process. The results of those simulations are as follows.

#### 4.4.2 Cylinder simulations

A simple cylinder (10 mm diameter, 50 mm height) was designed in Catia Software and was added as an initial geometry in Simufact for a thermomechanical analysis. Regarding mesh properties, a voxel size of 2 mm and a coarsening of level 2 was added. The initial density chosen was 99% since it was decided to start with a high porosity level and in the next simulations to decrease it. Fig.22(a-c) shows the predicted relative density after HIP by simulation.

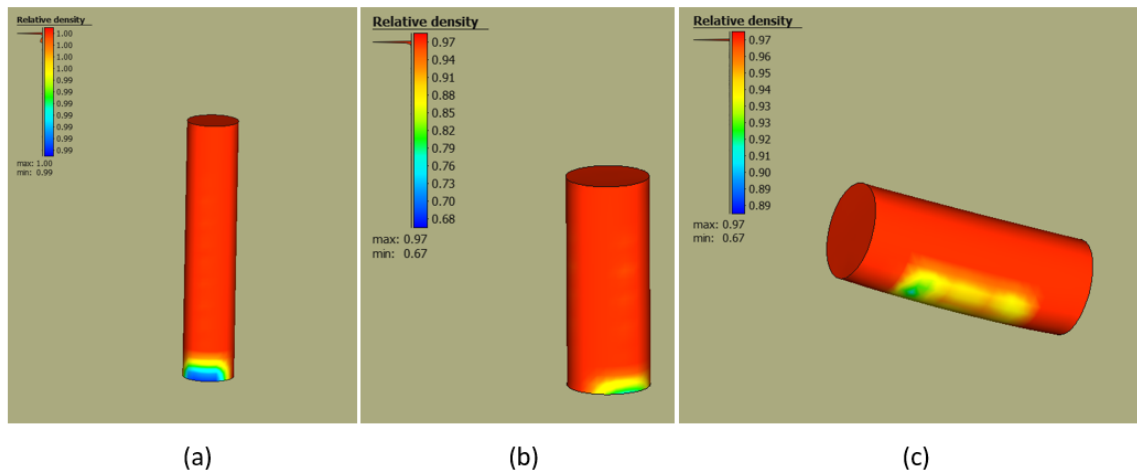


**Figure 22:** Relative density Results (a) First cylinder (b) Second cylinder printed vertically (c) Second cylinder printed horizontally

In Fig.22a, the simulation shows uniformity in density across the cylinder height apart from a particular spot near the base. Disregarding the base, relative density reaches 100% which means that porosity is eliminated in a broad part of the cylinder. A second simulation was conducted in the order to investigate the fluctuation in density at the base by decreasing the radius and the height of the cylinder (see Fig.22b). A diameter of 8mm and a height of 20mm are the dimensions of the new cylinder. In this simulation, some parameters changed such as the initial density of the part which was changed from 99% to 67.5%. This is because it was intended, firstly, to check this model in totally different density levels, one of them being very high and the other low and, secondly, the aim was to use similar parameters to other research projects to validate this project results with them. Also, more accuracy was required, and elements size was reduced for finer meshing so a voxel size of 1.4 was chosen.

As the Fig.22b depicts, this abnormal and intense density fluctuation was still taking place, but it was obvious that its size decreased. Simultaneously, the overall relative density reached 97% in the biggest part of the cylinder. After the second trial, the orientation was changed from vertical to horizontal (see Fig.22c) so as to investigate the model response to part orientation. It is seen that a horizontal orientation did not compromise in general, however, the region of lower relative density (also seen in Fig.22b) was still present but scattered across a larger region. Thus, the position and to some extent the area of the lower density region is influenced by cylinder orientation. In this part of the cylinder, one can observe that the relative density increases from 67% to 94%. The same initial relative density of 67% was simulated using ANSYS 2020 R2 in the study by [40], where a capsule filled with SS 316L powder was exposed to HIP conditions and was densified from 67% to 99%. In the particular study, porosity was eliminated in the biggest part of the object apart from some spots on the outer surface and, especially, in the corners where relative density could not exceed 89%. Simulating the same process with similar parameters in our case, the cylinders were almost densified. Applying the same initial density, the final

relative density did not exceed 97%. On the other hand, it can be observed that in the project's second simulation (See Fig.22b) where the cylinder is placed vertically, relative density does not exceed 88% in the corner created between the bottom and the main cylindrical core. This effect is very similar to the results described in [40].

Regarding the abnormal density fluctuation, the “canister effect” was a topic of discussion [50]. This phenomenon is activated in components consisting of sharp edges and sections of small dimensions. When these workpieces are exposed to HIP, the material in these places is unable to be densified since deformation levels are very low. This theory was rejected in this research because of two reasons.

Firstly, in the second simulation where the cylinder is printed vertically (See Fig.22b), the lack of densification shows up only in one side of the cylinder's sharp edges. Also, this looks like it covers only a small part of the bottom circle and not the whole bottom. Secondly, it was rejected because it can be easily observed that in the simulation results where the cylinder is placed horizontally Fig.22c), lack of densification appears to be located in an area that no sharp edges or corners exist. A more probable cause for these fluctuations could be connected to limitations in meshing and element size. The three simulations proved that element size played an important role in the whole process and especially in the first and second attempt. It is obvious that the lack of densification spot in Fig.22a is more intense and is spread in a larger surface while in Fig.22b) the intense fluctuation is decreased and is not scattered like the previous one. As it was mentioned in previous paragraphs, the second simulation was conducted using a finer mesh.

Finally, an error in the calculations and in the model is the main reason that led to this abnormal result. This error should be reported in Simufact Additive Support Service as a way to solve the issue.



# 5

## Conclusion and Future Work

*This chapter builds upon the results obtained in this thesis, aiming to answer the research questions and provide a basis for future research in the field. It presents insights and sets the stage for further investigations on the topic.*

### 5.1 Contributions of the Study

The present work aimed to add knowledge towards further industrialization of AM. This by investigating the challenges related to PBF-LB processing combined with HIP as means to lower costs and ensure high quality AM components. It paves the way for other researchers to explore porosity and take advantage of it, aiming to decrease printing time. The future idea is provided for tools regarding how one can predict shrinkage that occurs after HIP on a 3D-printed component, the final tolerances, and how much Finite Elements Method can contribute to it.

### 5.2 Summary of Key Findings

The questions that were investigated by this thesis project were related to the design of a manifold that is suitable in an additive manufacturing process and HIP. In addition, identification of relevant input parameters for accurate designs and simulations of component were studied to be suitable for HIP process.

To primarily address the initial research question, the objective was to develop a gas manifold and conduct simulations of the PBF-LB and HIP processes. To achieve this effectively, certain key parameters were identified as influential factors. These parameters include the gas flow rate during the design stage and the implementation of support structures during the printing stage. Regarding the gas manifold design, maintaining a constant flow rate led to minimal pressure drop among the designs in the GFA (See Fig.14), resulting in improved flow dynamics within the manifold. This characteristic is crucial in the manifold design process. Since it is an iterative design, the optimal combination can be achieved by further adjusting the flow rate based on the specific design requirements. The other factor is the support structures that is shown as affecting factor. By seeing the pre-print simulations (See Fig.17) it is very evident on the fact that how the design iterations are followed, showing the effect of support structures on a component.

Regarding the second research question addressed in this thesis, the simulation results obtained from GFA have demonstrated a reduction in pressure drop and an enhancement in the functionality of the gas manifold. Focusing on this aspect and utilizing design freedom, appropriate modifications were made to the design. Furthermore, the supports required for manufacturing this component using PBF-LB were significantly reduced (See Fig.19) and, as per the Materialise Magics software, eliminated altogether. Additionally, the Simufact simulations laid the groundwork for future system development that can be fine-tuned to obtain the mathematical outliers, specifically the relevant input parameters for shrinkage prediction during HIP, derived from the simulations. During the simulation of HIP on the cylinders and manifold, an unexpected fluctuation was observed on a small surface area. This irregular variation was reduced when the meshing element size (voxel) was decreased from 2 mm to 1.4 mm. Additionally, it was observed that support structures and porosity significantly impact productivity. By minimizing density, the component can be additively manufactured more rapidly using PBF-LB. However, it should be noted that post-processing is necessary to achieve a finished part with satisfactory mechanical properties.

When comparing this project's outcome with [40] that similar parameters have been followed, it was noticed that results related to relative density converge enough. The relative density of the cylinders after HIP reached 97% while in the other projects the relative density reached 99% or 100%. During the research, simulations were conducted on gas manifold and then on cylinder. The results that came out from both geometries simulations were almost the same and the irregular variation of relative density existed in cylinders and manifold, too. This was identified to be a meshing or internal computational issue and will be report the Simufact software team. This simulation data can be an origin point for some future work, which are explained in following section.

### 5.3 Future Work

In terms of future research opportunities, there are several areas that can be explored in relation to this topic.

- Firstly, further investigation can be conducted to apply the capabilities of simulation software such as Simufact Additive. Exploring the various tools and functionalities offered by the software can provide valuable insights into improving the accuracy and efficiency of simulations for additive manufacturing processes.
- The scope for testing the component, the theoretical results and simulation outcomes by prototyping the parts and validating the results using some intensive tools such as CT scanning helps in building a solid framework around the aspect of increasing the productivity. This can be continued for letting the customers understand how the process will affect based on their parameter

requirements.

- After the HIP process, the different densities of the components can be obtained and analyzed using Matlab software to predict the final shrinkage tolerances. The Simufact Additive simulations provided an estimation of the densification levels achieved during HIP. However, the precision of the FEM simulations can be further developed. Finer meshing results in more accurate information. Hence, the meshing process played a crucial role in the research, and there is potential for improving accuracy in future work.
- In addition, the data-driven approach in this research area can be developed along with above mentioned process. Machine learning techniques can be utilized to create meta models that accurately predict shrinkage and model the component for the desired outcome, along with other relevant parameters based on the initial component model. By incorporating a data-driven approach, the predictive capabilities of simulation models can be enhanced, allowing for the generation of more optimized models for additive manufacturing processes and the production of application-specific components. One potential application of this type of model is integrating tolerances based on an optimization model with customer data for finished parts. The combined data can then be fed into the simulation model to create spare parts that are customized exclusively based on the specific component requirements. These applications can be relevant to various industries, ranging from medical to aerospace.
- Finally, there is great potential for future research in weighing simulation software tools and advancing the data-driven approach for additive manufacturing simulations. These research possibilities can contribute to the development of more robust and efficient simulation models, ultimately enhancing the understanding and optimization of additive manufacturing processes.



# Bibliography

- [1] D. S. Thomas and S. W. Gilbert, “Costs and cost effectiveness of additive manufacturing: A literature review and discussion,” in *Additive Manufacturing: Costs, Cost Effectiveness and Industry Economics*, 2015.
- [2] B. Hüner *et al.*, *An Overview of Various Additive Manufacturing Technologies and Materials for Electrochemical Energy Conversion Applications*, 2022. DOI: 10.1021/acsomega.2c05096.
- [3] K. S. Prakash, T. Nancharaih, and V. V. Rao, “Additive Manufacturing Techniques in Manufacturing -An Overview,” in *Materials Today: Proceedings*, vol. 5, 2018. DOI: 10.1016/j.matpr.2017.11.642.
- [4] C. Lindemann, U. Jahnke, M. Moi, and R. Koch, “Analyzing product lifecycle costs for a better understanding of cost drivers in additive manufacturing,” in *23rd Annual International Solid Freeform Fabrication Symposium - An Additive Manufacturing Conference, SFF 2012*, 2012.
- [5] H. Chen, T. Cheng, Z. Li, Q. Wei, and W. Yan, “Is high-speed powder spreading really unfavourable for the part quality of laser powder bed fusion additive manufacturing?” *Acta Materialia*, vol. 231, 2022, ISSN: 13596454. DOI: 10.1016/j.actamat.2022.117901.
- [6] G. Allaire and B. Bogosel, “Optimizing supports for additive manufacturing,” *Structural and Multidisciplinary Optimization*, vol. 58, no. 6, 2018, ISSN: 16151488. DOI: 10.1007/s00158-018-2125-x.
- [7] F. Calignano and V. Mercurio, “An overview of the impact of additive manufacturing on supply chain, reshoring, and sustainability,” *Cleaner Logistics and Supply Chain*, vol. 7, 2023, ISSN: 27723909. DOI: 10.1016/j.clscn.2023.100103.
- [8] A. Leicht, M. Fischer, U. Klement, L. Nyborg, and E. Hryha, “Increasing the Productivity of Laser Powder Bed Fusion for Stainless Steel 316L through Increased Layer Thickness,” *Journal of Materials Engineering and Performance*, vol. 30, no. 1, 2021, ISSN: 15441024. DOI: 10.1007/s11665-020-05334-3.

- [9] M. Despeisse and T. Minshall, “Skills and education for additive manufacturing: A review of emerging issues,” in *IFIP Advances in Information and Communication Technology*, vol. 513, 2017. DOI: 10.1007/978-3-319-66923-6{\\_}34.
- [10] W. E. Frazier, “Metal Additive Manufacturing: A Review,” *Journal of Materials Engineering and Performance*, vol. 23, no. 6, pp. 1917–1928, Jun. 2014, ISSN: 1059-9495. DOI: 10.1007/s11665-014-0958-z.
- [11] C. Schwerz, F. Schulz, E. Natesan, and L. Nyborg, “Increasing productivity of laser powder bed fusion manufactured Hastelloy X through modification of process parameters,” *Journal of Manufacturing Processes*, vol. 78, pp. 231–241, Jun. 2022, ISSN: 15266125. DOI: 10.1016/j.jmapro.2022.04.013.
- [12] I. Yadroitsev, A. Du Plessis, I. Yadroitsava, and E. MacDonald, *Fundamentals of Laser Powder Bed Fusion of Metals: A volume in Additive Manufacturing Materials and Technologies*. 2021. DOI: <https://doi.org/10.1016/C2020-0-01200-4>.
- [13] N. Hopkinson, R. J. Hague, and P. M. Dickens, *Rapid Manufacturing: An Industrial Revolution for the Digital Age*. 2006. DOI: 10.1002/0470033991.
- [14] S. Bremen, W. Meiners, and A. Diatlov, “Selective Laser Melting,” *Laser Technik Journal*, vol. 9, no. 2, pp. 33–38, Apr. 2012, ISSN: 16137728. DOI: 10.1002/latj.201290018.
- [15] S. Chowdhury *et al.*, *Laser powder bed fusion: a state-of-the-art review of the technology, materials, properties & defects, and numerical modelling*, 2022. DOI: 10.1016/j.jmrt.2022.07.121.
- [16] D. Buchbinder, H. Schleifenbaum, S. Heidrich, W. Meiners, and J. Bültmann, “High power Selective Laser Melting (HP SLM) of aluminum parts,” in *Physics Procedia*, vol. 12, 2011. DOI: 10.1016/j.phpro.2011.03.035.
- [17] R. Singh *et al.*, “Powder bed fusion process in additive manufacturing: An overview,” in *Materials Today: Proceedings*, vol. 26, 2019. DOI: 10.1016/j.matpr.2020.02.635.
- [18] E. Atzeni and A. Salmi, “Economics of additive manufacturing for end-usable metal parts,” *International Journal of Advanced Manufacturing Technology*, vol. 62, no. 9-12, 2012, ISSN: 02683768. DOI: 10.1007/s00170-011-3878-1.
- [19] A. Gaikwad *et al.*, “Multi phenomena melt pool sensor data fusion for enhanced process monitoring of laser powder bed fusion additive manufacturing,” *Materials and Design*, vol. 221, 2022, ISSN: 18734197. DOI: 10.1016/j.matdes.2022.110919.

- 
- [20] W. Hearn, P. Harlin, and E. Hryha, “Development of powder bed fusion–laser beam process for AISI 4140, 4340 and 8620 low-alloy steel,” *Powder Metallurgy*, 2022, ISSN: 17432901. DOI: 10.1080/00325899.2022.2134083.
- [21] J. Wroe, “Introduction to Additive Manufacturing Technology: A Guide for Designers and Engineers,” *European Powder Metallurgy Association*, 2015.
- [22] M. Brandt, *Laser additive manufacturing: Materials, design, technologies, and applications*. 2016.
- [23] D. Höfflin, C. Sauer, A. Schiffler, and J. Hartmann, “Process Monitoring Using Synchronized Path Infrared Thermography in PBF-LB/M,” *Sensors*, vol. 22, no. 16, 2022, ISSN: 14248220. DOI: 10.3390/s22165943.
- [24] R. McCann *et al.*, *In-situ sensing, process monitoring and machine control in Laser Powder Bed Fusion: A review*, 2021. DOI: 10.1016/j.addma.2021.102058.
- [25] B. Song *et al.*, *Differences in microstructure and properties between selective laser melting and traditional manufacturing for fabrication of metal parts: A review*, 2015. DOI: 10.1007/s11465-015-0341-2.
- [26] R. Dogea, X. Yan, and R. Millar, “Additive manufacturing process design for complex aircraft components,” *International Journal of Advanced Manufacturing Technology*, vol. 123, no. 11-12, pp. 4195–4211, 2022. DOI: 10.1007/s00170-022-10413-x.
- [27] J. Jiang, X. Xu, and J. Stringer, *Support structures for additive manufacturing: A review*, 2018. DOI: 10.3390/jmmp2040064.
- [28] X. Peng, L. Kong, J. Y. H. Fuh, and H. Wang, *A review of post-processing technologies in additive manufacturing*, 2021. DOI: 10.3390/jmmp5020038.
- [29] V. Bhavar, P. Kattire, V. Patil, S. Khot, K. Gujar, and R. Singh, “A review on powder bed fusion technology of metal additive manufacturing,” in *Additive Manufacturing Handbook: Product Development for the Defense Industry*, 2017. DOI: 10.1201/9781315119106.
- [30] D. Grossin *et al.*, “A review of additive manufacturing of ceramics by powder bed selective laser processing (sintering / melting): Calcium phosphate, silicon carbide, zirconia, alumina, and their composites,” *Open Ceramics*, vol. 5, 2021, ISSN: 26665395. DOI: 10.1016/j.oceram.2021.100073.
- [31] J. P. Pragana *et al.*, “Influence of processing parameters on the density of 316L stainless steel parts manufactured through laser powder bed fusion,” *Proceedings of the Institution of Mechanical Engineers, Part B: Journal of*

- Engineering Manufacture*, vol. 234, no. 9, 2020, ISSN: 20412975. DOI: 10.1177/0954405420911768.
- [32] L. Gasman, "Additive aerospace considered as a business," in *Additive Manufacturing for the Aerospace Industry*, 2019. DOI: 10.1016/B978-0-12-814062-8.00017-0.
- [33] H. Schleifenbaum, A. Diatlov, C. Hinke, J. Bültmann, and H. Voswinckel, "Direct photonic production: Towards high speed additive manufacturing of individualized goods," *Production Engineering*, vol. 5, no. 4, 2011, ISSN: 09446524. DOI: 10.1007/s11740-011-0331-0.
- [34] C. Du *et al.*, "Pore defects in Laser Powder Bed Fusion: Formation mechanism, control method, and perspectives," *Journal of Alloys and Compounds*, vol. 944, p. 169215, May 2023, ISSN: 0925-8388. DOI: 10.1016/J.JALLCOM.2023.169215.
- [35] Y. Mao, J. Yuan, Y. Heng, K. Feng, D. Cai, and Q. Wei, "Effect of hot isostatic pressing treatment on porosity reduction and mechanical properties enhancement of 316L stainless steel fabricated by binder jetting," *Virtual and Physical Prototyping*, vol. 18, no. 1, 2023, ISSN: 17452767. DOI: 10.1080/17452759.2023.2174703.
- [36] W. H. Kan *et al.*, *A critical review on the effects of process-induced porosity on the mechanical properties of alloys fabricated by laser powder bed fusion*, 2022. DOI: 10.1007/s10853-022-06990-7.
- [37] R. Snell *et al.*, "Methods for Rapid Pore Classification in Metal Additive Manufacturing," *JOM*, vol. 72, no. 1, 2020, ISSN: 15431851. DOI: 10.1007/s11837-019-03761-9.
- [38] K. Yuasa *et al.*, "Influences of powder characteristics and recoating conditions on surface morphology of powder bed in metal additive manufacturing," *International Journal of Advanced Manufacturing Technology*, vol. 115, no. 11-12, 2021, ISSN: 14333015. DOI: 10.1007/s00170-021-07359-x.
- [39] N. L. Loh and K. Y. Sia, "An overview of hot isostatic pressing," *Journal of Materials Processing Tech.*, vol. 30, no. 1, 1992, ISSN: 09240136. DOI: 10.1016/0924-0136(92)90038-T.
- [40] S. Sobhani, M. Albert, D. Gandy, A. Tabei, and Z. Fan, "Design Optimization of Hot Isostatic Pressing Capsules," *Journal of Manufacturing and Materials Processing*, vol. 7, no. 1, 2023, ISSN: 25044494. DOI: 10.3390/jmmp7010030.
- [41] S. Sahoo, B. B. Jha, and A. Mandal, "Powder metallurgy processed TiB<sub>2</sub>-reinforced steel matrix composites: a review," *Materials Science and Tech-*

- nology*, vol. 37, no. 14, pp. 1153–1173, Sep. 2021, ISSN: 0267-0836. DOI: 10.1080/02670836.2021.1987705.
- [42] *Hot Isostatic Pressing— Theory and Applications*. 1992. DOI: 10.1007/978-94-011-2900-8.
- [43] M. Abouaf, J. L. Chenot, G. Raisson, and P. Bauduin, “Finite element simulation of hot isostatic pressing of metal powders,” *International Journal for Numerical Methods in Engineering*, vol. 25, no. 1, 1988, ISSN: 10970207. DOI: 10.1002/nme.1620250116.
- [44] R. Davis, “Hot Isostatic Pressing,” in *Concise Encyclopedia of Advanced Ceramic Materials*, Elsevier, 1991, pp. 210–215. DOI: 10.1016/B978-0-08-034720-2.50061-7.
- [45] B. Elguezabal, J. Alkorta, and J. M. Martínez-Esnaola, “Study of Astroloy powder compaction at high temperature under hydrostatic load using finite elements,” *Powder Technology*, vol. 381, pp. 92–100, Mar. 2021, ISSN: 0032-5910. DOI: 10.1016/J.POWTEC.2020.12.001.
- [46] C. Van Nguyen, Y. Deng, A. Bezold, and C. Broeckmann, “A combined model to simulate the powder densification and shape changes during hot isostatic pressing,” *Computer Methods in Applied Mechanics and Engineering*, vol. 315, pp. 302–315, Mar. 2017, ISSN: 0045-7825. DOI: 10.1016/J.CMA.2016.10.033.
- [47] R. P. Guo, L. Xu, J. Wu, Z. G. Lu, and R. Yang, “Simulation of Container Design for Powder Metallurgy Titanium Components Through Hot-Isostatic-Pressing,” in *Materials Science Forum*, vol. 817, Trans Tech Publications Ltd, 2015, pp. 610–614, ISBN: 9783038353966. DOI: 10.4028/www.scientific.net/MSF.817.610.
- [48] Per Lindström, “Improved CWM platform for modelling welding procedures and their effects on structural behaviour Per Lindström,” *University West*, vol. 2015 No.6, ISSN: 2015-3154.
- [49] A. Du Plessis *et al.*, “Productivity enhancement of laser powder bed fusion using compensated shelled geometries and hot isostatic pressing,” *Advances in Industrial and Manufacturing Engineering*, vol. 2, p. 100 031, May 2021, ISSN: 26669129. DOI: 10.1016/j.aime.2021.100031. [Online]. Available: <https://linkinghub.elsevier.com/retrieve/pii/S2666912921000015>.
- [50] A. M. Abdelhafeez and K. E. Essa, “Influences of Powder Compaction Constitutive Models on the Finite Element Simulation of Hot Isostatic Pressing,” in *Procedia CIRP*, vol. 55, Elsevier B.V., 2016, pp. 188–193. DOI: 10.1016/j.procir.2016.07.025.



# A

## Appendix - Design characteristics

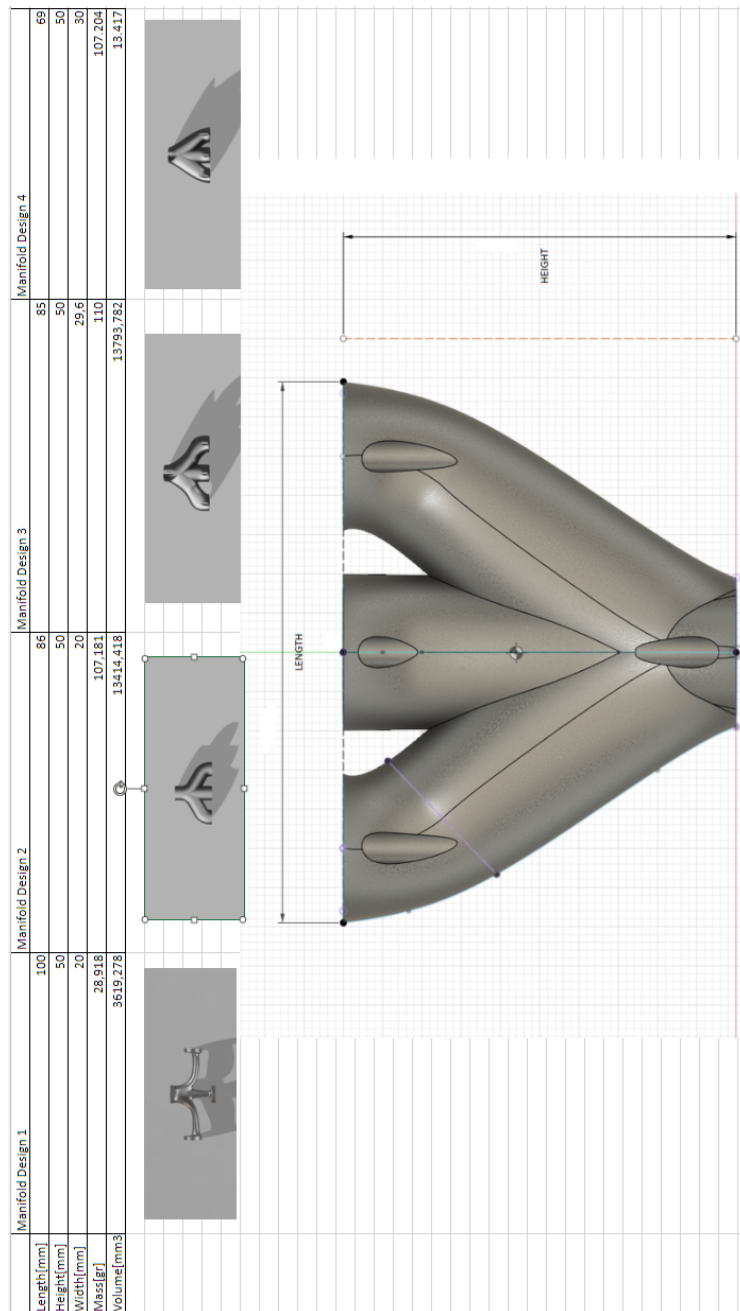
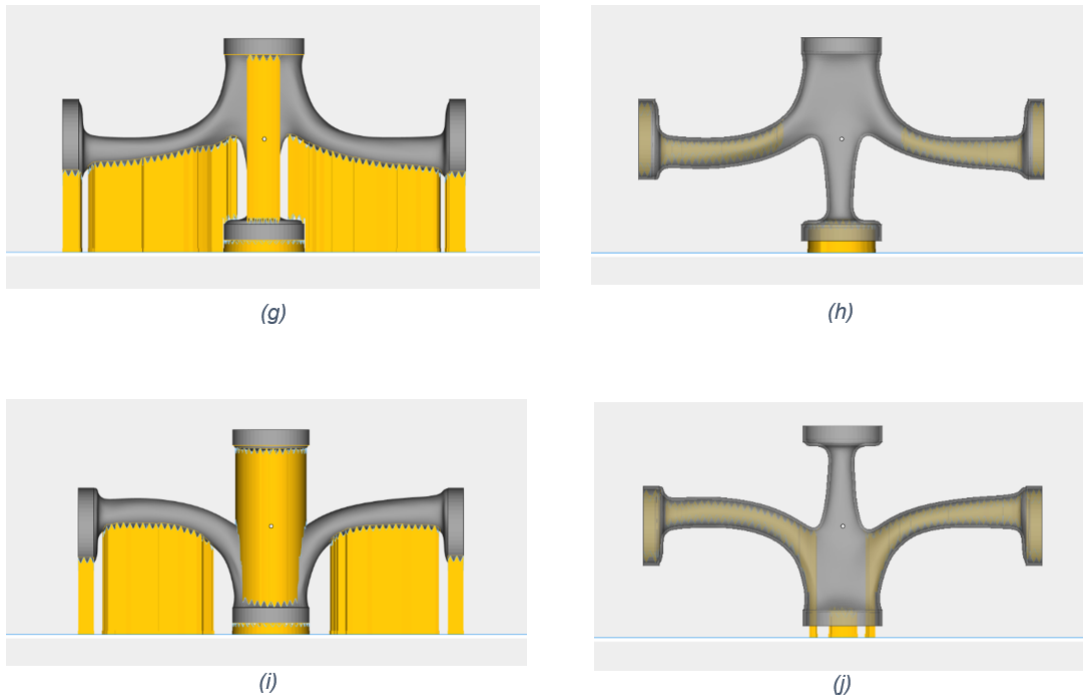


Figure 23: Design Iterations-Dimensions







**Figure 25:** (g) 4th orientation, Outer supports (h) 4th orientation, Inner supports (i) 5th orientation, Outer supports (j) 5th orientation, Inner supports

# C

## Appendix - GFA - 2

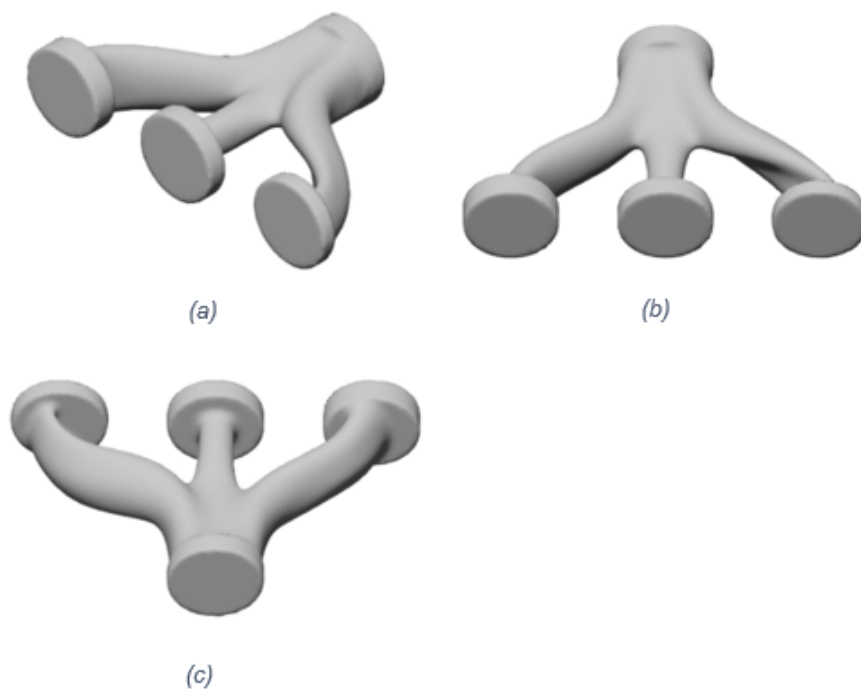


**Figure 26:** Manifold GFA-2 Multiple Angles (a) 1st angle (b) 2nd angle (c) 3rd angle



# D

## Appendix - Build Orientations

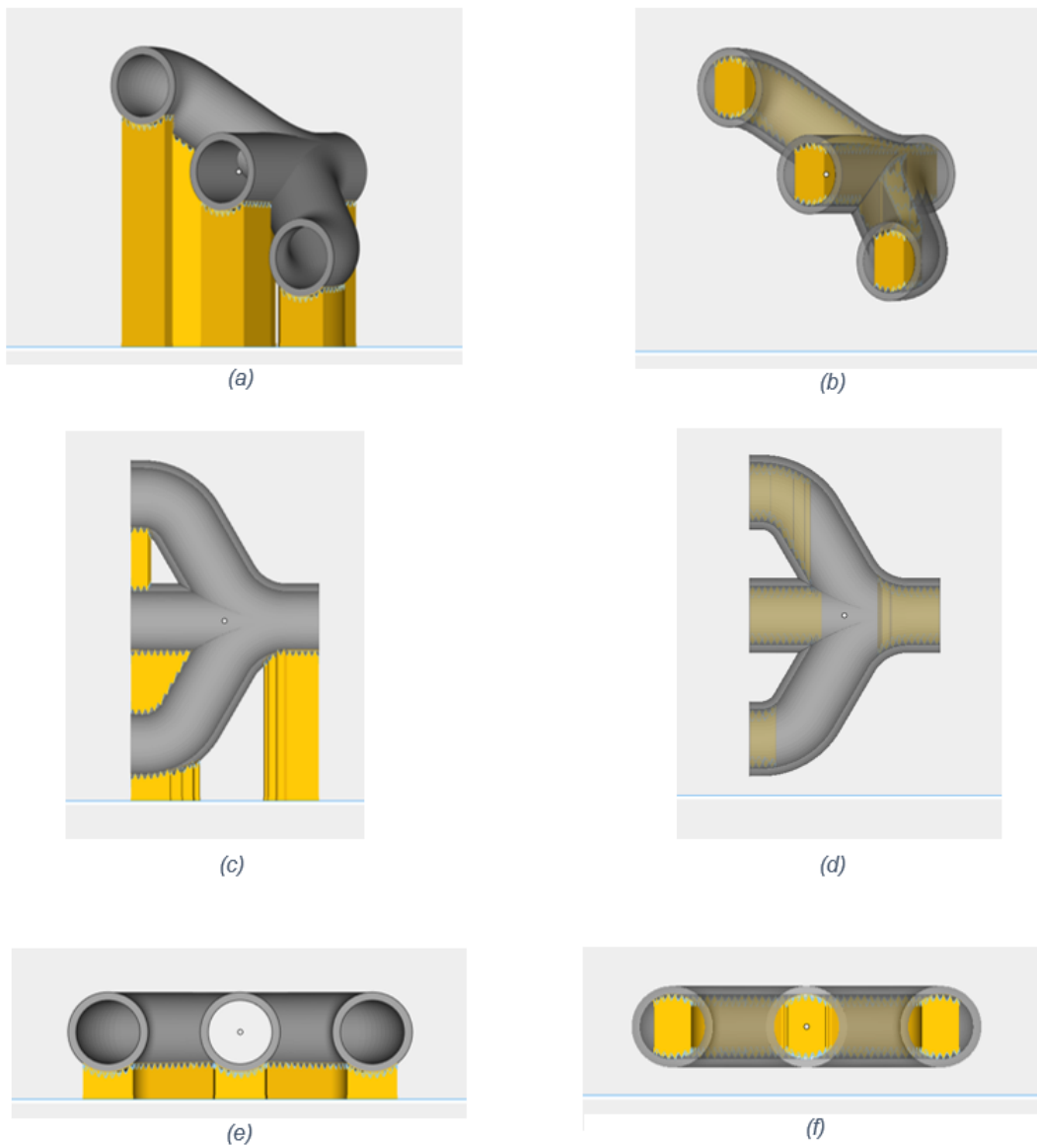


**Figure 27:** (a) 1st orientation, Outer supports (b) 1st orientation, Inner supports (c) 2nd orientation, Outer supports (d) 2nd orientation, Inner supports (e) 3rd orientation, Outer supports (f) 3rd orientation, Inner supports

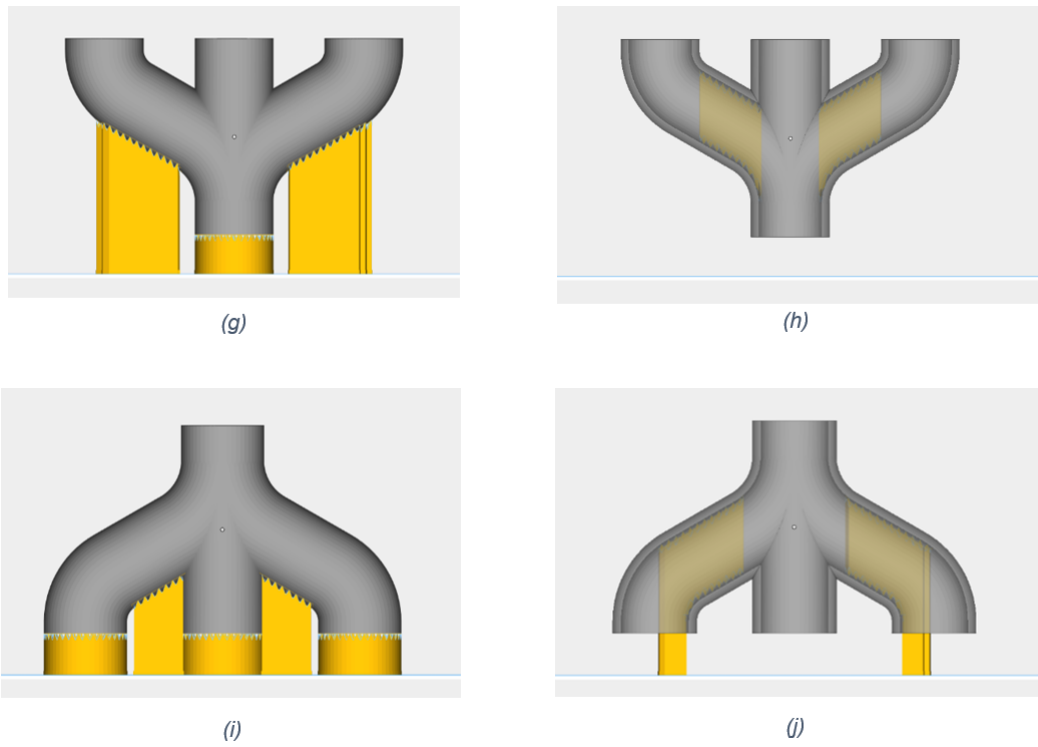


**Figure 28:** (a) 1st orientation, Outer supports (b) 1st orientation, Inner supports  
(c) 2nd orientation, Outer supports (d) 2nd orientation, Inner supports (e) 3rd  
orientation, Outer supports (f) 3rd orientation, Inner supports

DEPARTMENT OF SOME SUBJECT OR TECHNOLOGY  
CHALMERS UNIVERSITY OF TECHNOLOGY  
Gothenburg, Sweden  
[www.chalmers.se](http://www.chalmers.se)



**CHALMERS**  
UNIVERSITY OF TECHNOLOGY